Engineering 7 (2021) 564–580

Contents lists available at ScienceDirect

Engineering

journal homepage: www.elsevier.com/locate/eng

Research
Green Chemical Engineering: Soft Matter—Review

Advances in Soft Materials for Sustainable Electronics

Moon Jong Han [a], Dong Ki Yoon [a,b,c,*]

[a] Graduate School of Nanoscience and Technology, Korea Advanced Institute of Science and Technology, Daejeon 34141, Republic of Korea
[b] Department of Chemistry, Korea Advanced Institute of Science and Technology, Daejeon 34141, Republic of Korea
[c] KAIST Institute for NanoCentury, Korea Advanced Institute of Science and Technology, Daejeon 34141, Republic of Korea

ARTICLE INFO

Article history:
Received 1 October 2020
Revised 8 December 2020
Accepted 8 February 2021
Available online 18 April 2021

Keywords:
Sustainable
Biodegradable
Soft materials
Organic electronics

ABSTRACT

In the current shift from conventional fossil-fuel-based materials to renewable energy, ecofriendly materials have attracted extensive research interest due to their sustainability and biodegradable properties. The integration of sustainable materials in electronics provides industrial benefits from wasted bio-origin resources and preserves the environment. This review covers the use of sustainable materials as components in organic electronics, such as substrates, insulators, semiconductors, and conductors. We hope this review will stimulate interest in the potential and practical applications of sustainable materials for green and sustainable industry.

1. Introduction

A recent trend in electronic devices is to develop specially designed organic materials that exhibit high flexibility, sometimes including mechanical stretchability, which have been considered for practical or potential applications ranging from wearable electronics to applications in mobile health, sports, and more [1]. Much of the interest in the use of organic material is associated with the desire to design electronic components that are ecofriendly and biocompatible, or even metabolizable [2–5]. The adoption of material derived from nature is a primary concern for both society and industry. This aim conflicts with the ever-increasing volume of electronic waste, which was estimated to be 5.0×10^7 Mt in 2018 [6]. In particular, plastic expenditure and waste have been presenting enormous problems in recent times. For example, polyethylene is presently at the peak of universal consumption, at about 275 Mt in 2015, and is widely used in everyday substances including plastic bags, toys, and packing materials [7]. Due to the greater demands of emerging industries and the current coronavirus disease 2019 (COVID-19) in 2020, more plastics are being consumed, and their full degradation will take over 500 years [8,9].

Therefore, inspiration from nature has led to explorations in biocompatible electronics, prompting the development of organic electronics that naturally break down when their use is over [10]. A broad area of sustainable organic materials originating from animals, plants, and bacteria, such as chitin, cellulose, starch, and various kinds of proteins, have been studied [11–24], and are generally adopted in various applications such as coating materials, biomedical applications, and so on. With increasing demands for sustainable devices, the question of how to integrate non-petroleum and plastics-related exotic materials with the present standards of living is coming under scrutiny. Sustainable materials with superior biodegradability have attracted a great deal of attention in terms of being integrated with devices in order to benefit from bio-origin materials while preserving the environment. However, integrating sustainable materials in electronic devices with a high-efficiency output is a continued obstacle. Nevertheless, persistent environmental concerns have rationalized the use of organic electronics in substrates, the dielectric layer, and semiconducting materials [25].

Hence, this review aims to provide a brief overview of sustainable materials for use in degradable circuit boards and organic electronics, covering the latest developments in this field. In this review, organic soft materials are classified based on function, such as ① substrates and insulators, ② semiconductors, and ③ conductors. We predict that life will be as comfortable and safe with highly deformable and biodegradable electronics integrated everywhere—in clothes and with our

* Corresponding author.
E-mail address: nandk@kaist.ac.kr (D.K. Yoon).

https://doi.org/10.1016/j.eng.2021.02.010

bodies in the near future—just as we are currently familiar with tablet computers and smartphones.

2. Passive and active components

2.1. Substrates and dielectric layers

2.1.1. Paper and silk

Various materials originating from nature have been considered to be appropriate substrates for organic electronics due to their numerous advantages, including economic benefits, biocompatibility, and nontoxicity. One of the most familiar and classical organic substrates is paper, which is made from plants or wood-derived cellulose. The outstanding physical characteristics of cellulose make it possible to cover large areas and enable the mass production of paper. Paper is superior to other deformable passive materials due to its economical price, at approximately 0.2 USD·m^{-2}, excellent flexibility, and roll-to-roll (R2R) fabrication capability at a fast process speed of about 25 m·s^{-1} [26]. In addition to its use in typical packaging and storage applications, paper has been developed for use as a substrate for various unconventional forms. Organic thin-film transistor (OTFT)-based circuits have been fabricated on paper and have demonstrated flexibility and specific results comparable to those of conventional polymer substrates (Fig. 1(a)) [27–29]. Low-voltage-driven OTFTs have been achieved on banknotes for applications in anti-counterfeiting. OTFTs could be fabricated on paper operating under less than 2 V with mobilities of about 0.3 cm^2·V^{-1}·s^{-1}, regardless of banknote paper's surface roughness. Yun et al. [30], Shao et al. [31], Ha et al. [32], Casula et al. [33], and Martins et al. [34] utilized low power-driven complementary metal–oxide semiconductor (CMOS) inverters based on a paper substrate. Fig. 1(b) [29] shows a photograph of a CMOS inverter operating in accordance with input-voltage (V_{in}). In addition, paper substrates have been applied to other opto-electrical devices, including organic photovoltaics (OPVs) and thermochromic displays [35–37]. In particular, the advanced performance of OPVs has been demonstrated via full R2R printing by means of a solution process using flexographic and gravure methods. The device has an inverted configuration, such as a printed ZnO/Zn bottom and a conducting polymer top electrode based on economical materials with a low-temperature solution process (Fig. 1(c) [37]). Another example is the use of low-temperature chemical vapor deposition (CVD) onto paper for photovoltaics; the device consists of conducting polymer electrodes, an active organic layer, and reflective back electrodes, as shown in Fig. 1(d) [38]. This work demonstrated arrays of OPV devices that could be folded without degradation of the electrical characteristics, demonstrated through repeated folding tests.

Silk is another natural material with a long history that has been applied in the dielectric layer and as an electronic device

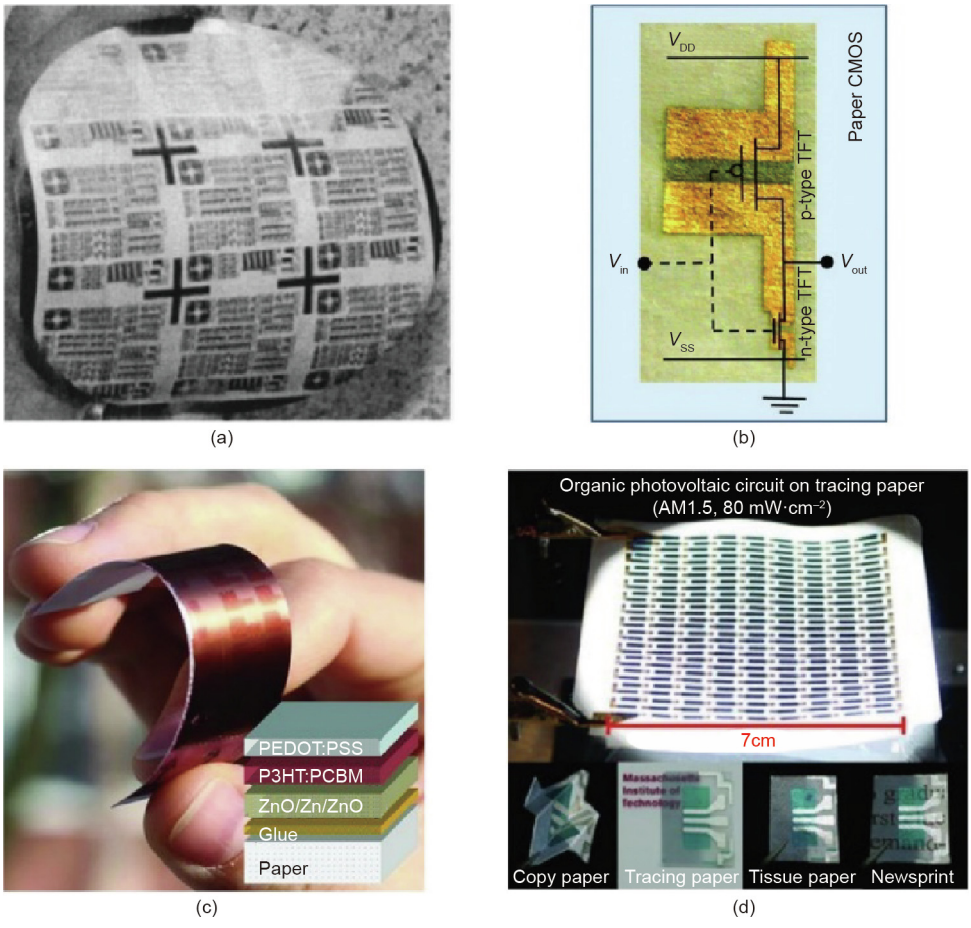

Fig. 1. Paper-substrate-based electronic devices. (a) OTFT arrays fabricated on a paper substrate; (b) a CMOS inverter circuit on a paper substrate; (c) a flexible, solution-processed OPV on paper with the device configuration (bottom right corner); (d) image of CVD-based solar cells on semitransparent paper. TFT: thin-film-transistor; V_{in}: input-voltage; V_{out}: output-voltage; V_{DD}: voltage drain to drain; V_{SS}: voltage source to source; PEDOT:PSS: poly(3,4-ethylenedioxythiophene) system doped with polyanionic poly(styrene sulfonate); P3HT:PCBM: poly(3-hexylthiophene):(6,6)-phenyl-C_{61}-butyric acid methyl ester. (a) Reproduced from Ref. [27] with permission of AIP Publishing, ©2004; (b) reproduced from Ref. [29] with permission of Wiley-VCH, ©2011; (c) reproduced from Ref. [37] with permission of Wiley-VCH, ©2011; (d) reproduced from Ref. [38] with permission of Wiley-VCH, ©2011.

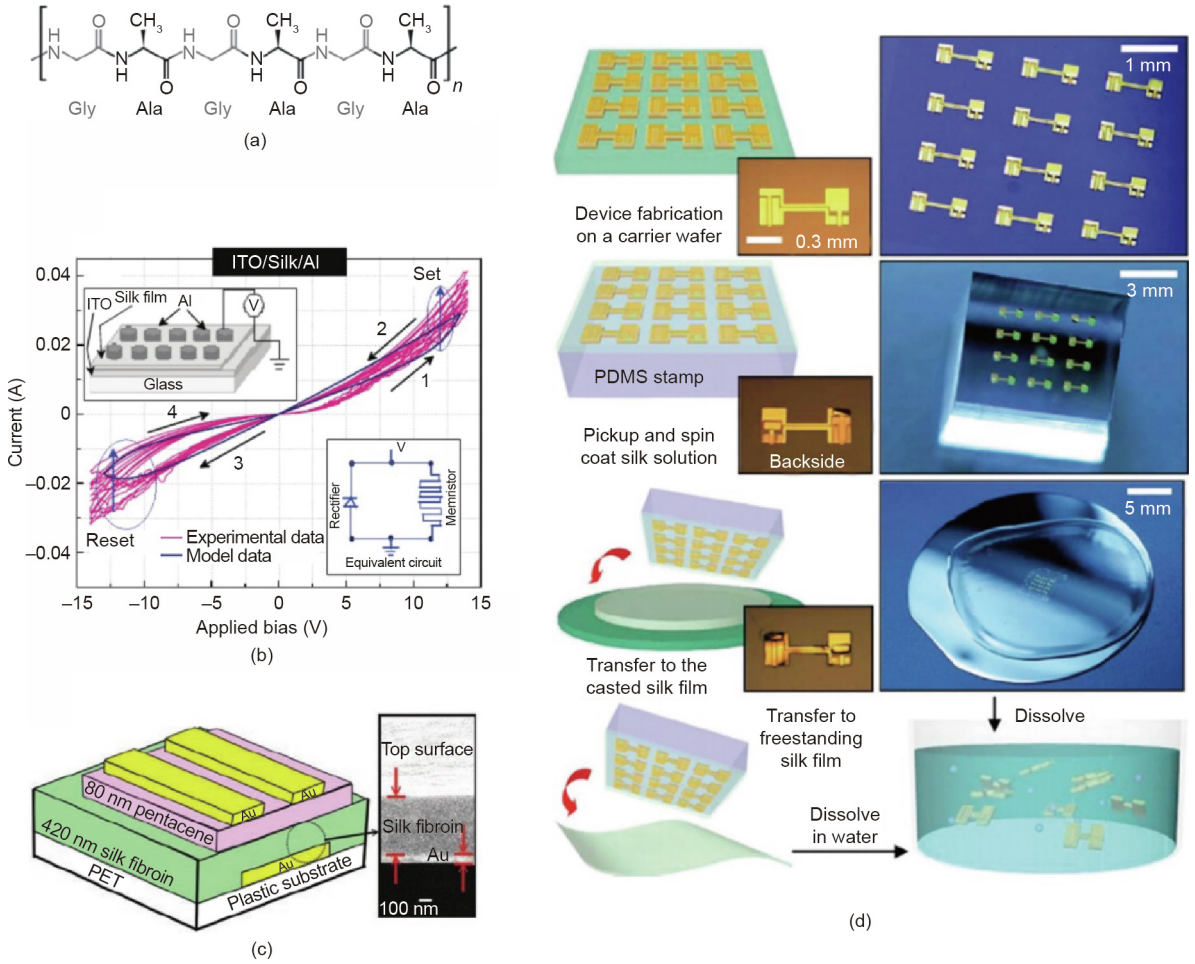

Fig. 2. Dielectric layer and substrates based on silk. (a) Chemical structure of silk fibroin; (b) bio-memory resistor based on silk fibroin protein showing reversible and nonvolatile properties; (c) solution-processed silk fibroin films as the dielectric layer in flexible OTFTs; (d) bioresorbable silk substrates for the transfer of a sensor array onto brain tissue. ITO: indium-tin-oxide; PDMS: poly(dimethylsiloxane); PET: polyethylene terephthalate. (b) Reproduced from Ref. [40] with permission of Wiley-VCH, ©2012; (c) reproduced from Ref. [41] with permission of Wiley-VCH, ©2011; (d) reproduced from Ref. [44] with permission of Springer Nature, ©2010.

substrate. Fundamentally, silk is a polypeptide polymer consisting of fibroin and sericin. Fibroin has repeated glycine, serine, and alanine units, which enhance the mechanical robustness due to interchain hydrogen bonding (Fig. 2(a)) [39]. Hota et al. [40] manipulated bio-origin silk fibroin to make a transparent bio-memory resistor and analyzed the device's endurance and retention characteristics. As shown in Fig. 2(b) [40], metal–insulator–metal capacitors based on silk fibroin exhibited memory resistor functionality with simultaneous rectifying properties. In addition, silk was applied as an efficient gate insulator layer on a polyethylene terephthalate (PET) substrate (Fig. 2(c)), exhibiting a mobility of about 23 $cm^2 \cdot V^{-1} \cdot s^{-1}$ with low-voltage operation [41]. Another example of silk being applied as a dielectric layer was demonstrated by Capelli et al. [42], whose organic light-emitting transistors based on silk yielded a light emission of 100 nW. Chang et al. [43] made use of spider silk as a polyelectrolyte dielectric layer in OTFTs based on a pentacene semiconductor and investigated the hydration of the silk dielectric with respect to reproducibility under different levels of humidity. In addition, various research groups have investigated the characteristics of silk, which include deformability and outstanding mechanical properties. Kim et al. [44] demonstrated metal electrodes with the bioresorbable properties of silk (Fig. 2(d)), and showed the transfer printing process. In the fabrication sequence, metal–oxide field effect transistors (FETs) were fabricated on a poly(methyl methacrylate) temporary substrate. Next, the devices were fished on a poly(dimethylsiloxane) substrate. As a result, the electrodes were transferred to the silk film above a silicon substrate, resulting in resorbable elements that could be safely implanted into the body, and in which the degree of crystallinity was tuned to modulate transient times. In subsequent research, Hwang et al. [45] demonstrated biomedical applications based on electronics interacting with living tissue, with controlled transient times and resolution.

2.1.2. Cellulose and cellulose derivatives

Cellulose is a famous example of the abundant biopolymers available in nature. It is superior to non-carbohydrate lignin, and is one of the most significant biomass materials. Cellulose is a well-ordered material that can form stable nanostructures, in which van der Waals interactions and hydrogen bonding between the oxygen atoms and hydroxyl groups of neighboring molecules result in lateral packing. This packing results in the formation of aggregates or nanofibrils into larger microfibrils, whose crystalline structure and amorphous domains have been explored in detail. Furthermore, cellulose nanocrystals (CNCs) can be extracted from the crystalline regions of cellulose, and possess the unique properties of a high aspect ratio, high mechanical strength, and liquid crystallinity [46–51]. By taking advantage of the template ability

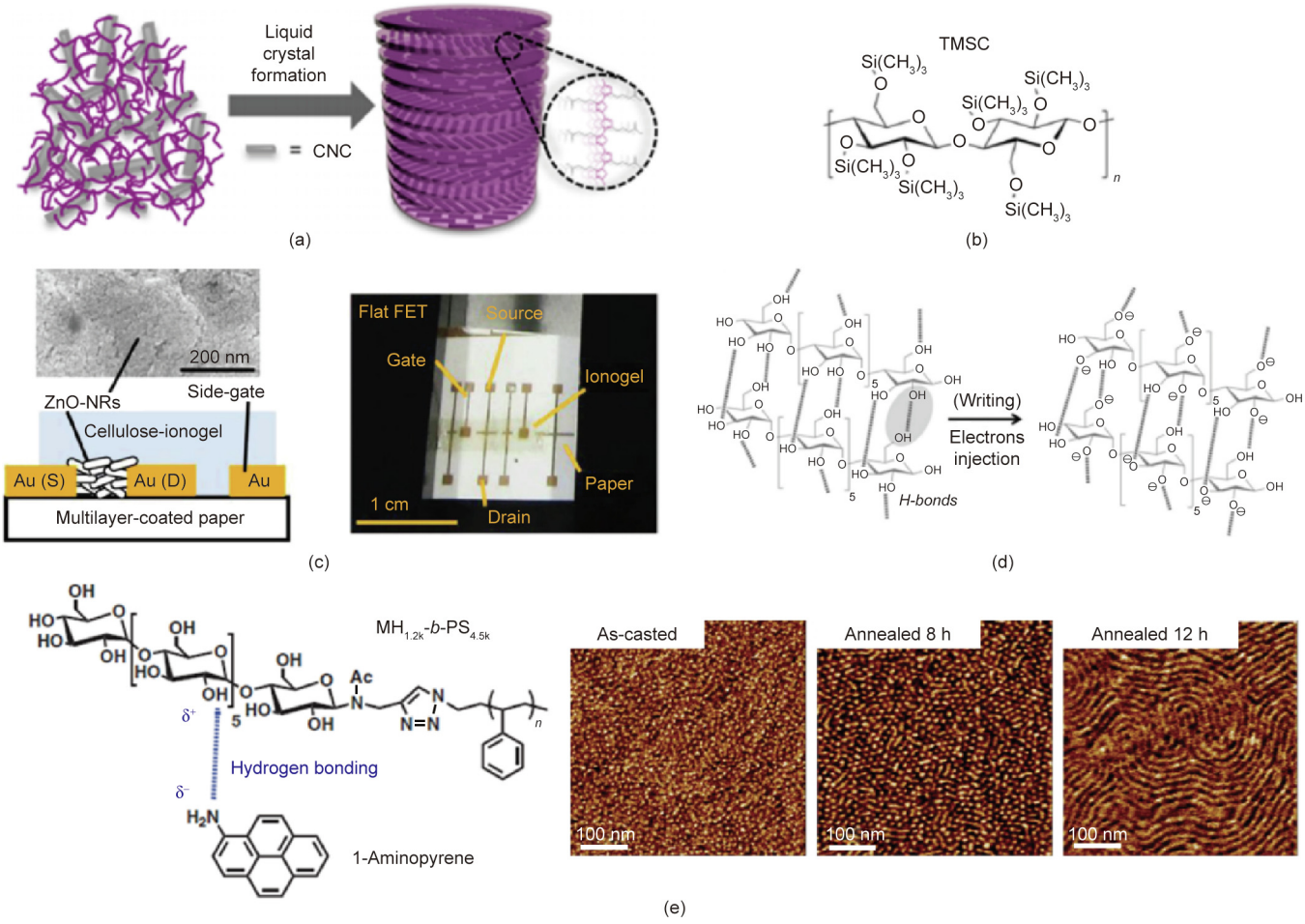

Fig. 3. LC and dielectric properties of cellulose moieties. (a) Orientation control of a semiconducting polymer assisted by a cellulose-based LC template; (b) schematic illustration of OTFTs based on a cellulose-derivative dielectric layer with the chemical structure of TMSC; (c) bending tests of a cellulose ion gel-based TFT configuration with electrical properties; (d) OTFT memory device with a maltoheptaose (MH) dielectric layer and proposed memory mechanisms; (e) chemical structure of MH-*b*-PS diblock copolymer with OTFT memory device properties depending on molecular configuration. NR: nanorod. (a) Reproduced from Ref. [52] with permission of the American Chemical Society, ©2017; (b) reproduced from Ref. [54] with permission of Wiley-VCH, ©2015; (c) reproduced from Ref. [55] with permission of Wiley-VCH, ©2013; (d) reproduced from Ref. [56] with permission of Wiley-VCH, ©2015; (e) reproduced from Ref. [57] with permission of Wiley-VCH, ©2014.

of CNCs based on their liquid crystal (LC) characteristics, it was possible to generate a long-range ordered semiconducting polymer, poly[3-(potassium-4-butanoate) thiophene-2,5-diyl] (PPBT) (Fig. 3(a)) [52]. In a mixed solution state, PPBT molecules were combined with an LC template of CNCs, resulting in an ordered state with oriented domains. Thus, the existence and packing of CNCs exhibiting an LC phase resulted in enhanced π–π stacking of the PPBT molecules. The PPBT polymer chains incorporated with the CNC host and followed its organization within the confinement of the CNC aggregates [53]. To minimize the excluded volume in this confined geometry, the PPBT chains aggregated and became oriented, which maximized the translational entropy by sacrificing the orientational entropy. Moreover, a chirality within the PPBT/CNC complex was analyzed by means of circular dichroism measurement, suggesting that the polymer chains mimicked the chirality of the helicoidal twisted nematic LC host, the CNCs.

Furthermore, the functionalization of cellulose grants it dielectric properties in bioelectronics. Attaching functional groups to impart solution processability to the cellulose derivative trimethylsilyl cellulose (TMSC) allowed it to act as an ultrathin dielectric film for thin-film transistors (TFTs) (Fig. 3(b)) [54]. A hybrid organic/inorganic dielectric layer based on aluminum oxide, Al_2O_3, and TMSC was used as a capping layer for device fabrication. Using the dielectric layer, TFTs based on p- and n-type semiconductors could operate at about 15 V, exhibiting charge-carrier mobilities of about 0.1 and 0.6 $cm^2 \cdot V^{-1} \cdot s^{-1}$, respectively. The TMSC-based device showed negligible electrical hysteresis due to the low degree of shallow traps. Another study utilized cellulose-based ion gel as a suitable gate dielectric layer to design electrolyte-gated OTFTs, as demonstrated in Fig. 3(c) [55]. The electrolyte thin film was ionically conductive with high electronic insulation and flexibility, resulting in superior dielectric characteristics and a high capacitance ranging from about 4.5 to 15.5 $\mu F \cdot cm^{-2}$. The schematic illustration in Fig. 3(c) shows an ion gel electrolyte-gated TFT based on a ZnO nanorods semiconductor, turning on at 0.8 V and exhibiting an on/off ratio of about 100, as extracted from transfer curves.

In addition, the cellulose-based layer showed good dielectric performance in a memory device due to the existence of induced charge carriers at the interface between the dielectric and the semiconductor. Chiu et al. [56] made use of the functional groups of biomaterials to trap or accumulate the charge carriers generated at the interfaces in order to advance the device's properties. Moreover, a multiple charge-storage property was exhibited by numerous hydroxyl groups-based polysaccharides with α-glucan

derivatives, showing the close interface or the polysaccharide texture. As shown in Fig. 3(d) [56], some polysaccharides, such as maltoheptaose (MH), dextran, and polysucrose, were applied to transistors under the semiconductor. Under a positive gate voltage, there was a considerable threshold voltage change in the transfer characteristic, which was maintained. This implies that charge carriers generated by an electric field might have accumulated in the polysaccharide surface under the gate voltage. Therefore, the results showed a high drain current with nonvolatile and stable-retention properties derived from the strong charge trapping. The hydroxyl groups deprotonate when electrons are transported from the semiconductor, inducing oxygen ions. The subsequent hydroxylate anions may strengthen the hydrogen bonding to enhance the storage of the polysaccharides' electron charges. Furthermore, a polysaccharide with an organic semiconductor interacted with a block copolymer electret, maltoheptaose-*block*-polystyrene (MH-*b*-PS), in a memory device (Fig. 3(e)) [57]. The electron-trapping property of horizontally aligned cylindrical MHs was superior than that of random-sphere conditions (as-coated), vertically oriented cylinder structures (thermal annealed at 8 h), or horizontally oriented cylinder structures (thermal annealed at 12 h) because the hydroxyl groups were within an active contact range. Electrical properties were further increased using the hydrogen bonding between 1-aminopyrene and the hydroxyl groups within the MH derivatives. In general, this configuration afforded an outstanding flash memory, exhibiting a wide memory window (~50 V), retention times of about 1×10^4 s, an on-current/off-current (I_{on}/I_{off}) of about 1×10^5, and stable reversibility of about 250 cycles. Therefore, the results showed that polysaccharide functional groups can modulate the electrical properties of sustainable transistor memory devices with high performance.

2.1.3. Resins, gelatin, albumen, and Aloe vera

A resin is a bio-origin material derived from plants and animals. For example, plant resins include sap or viscous exudates. Resins are hydrophobic volatile and nonvolatile terpenoid compounds with or without phenolic secondary complexes existing within or above the plant surface. These compounds have attracted research attention due to their medicinal applications, their application in the industrial production of varnishes and lacquers, and their use in incense and perfume. For example, amber and copal, which originate from plants, are known to have a high insulation capacity. There are also animal-derived resins. For example, shellac is an animal-derived resin extracted from the insect *Tachardia lacca*. It was used as a folder for stereo records with approximately 80 revolutions per minute (rpm), but is now more commonly used as a barrier to prohibit the decrease of moisture within citrus fruits, and is also applied to therapeutic capsules for floating the above unaffected regions of the gastrointestinal portion and searching the province [58]. Goswami [59] investigated the natural resin shellac and Irimia-Vladu et al. [60] used shellac as the dielectric layer in OTFTs. Alcoholic solvents were used to dissolve the shellac flakes, and the solution process, such as drop and spin coating, generated different thicknesses of the thin films. Post-crosslinking was performed using a heating process that did not exceed about 100 °C, inducing remarkable surface smoothness. Furthermore, shellac dielectric-based OTFTs were fabricated and exhibited outstanding smoothness of the film without the relaxation of dipolar molecules or ions. Fig. 4(a) [60] shows the schematic configuration of C_{60}- and pentacene-based OTFTs with a shellac dielectric layer. The electrical properties demonstrated negligible hysteresis, suggesting that the density of the trapped electrons or holes is trivial. Many kinds of resins derived from plants remain to be investigated for use in electronic devices.

Gelatin has a long history as a commonly adopted material. For example, the ancient Egyptians heated bone and animal leather to use native collagen as an adhesive. For the first time in 2010, gelatin was applied in a completely biodegradable and biocompatible organic field effect transistor (OFET) based on a gelatin substrate [61]. A smooth surface of stiff gelatin exhibits a root-mean-square (RMS) roughness of about 30 nm. For application in organic electronics, minimized roughness of the substrate is essential, as the roughness influences the fabrication processes of the films above, affecting the function of each dielectric and semiconductor, and of the electrode layers' interface. Fig. 4(b) [61] shows a typical gelatin-based electronic device, in which a tetratetracontane layer placed by thermal evaporation onto the gelatin film exhibits passivation and minimizes hysteresis, with low leakage currents. Another interesting application of gelatin is its use in polymer complexes.

Recently, there has been a need for elements that can tune the degradation and solubility in biomedical electronics and degradable bio-devices. Acar et al. [62] demonstrated that a gelatin filler with poly(vinyl alcohol) (PVA) as a polymer complex could improve the mechanical characteristics of an dielectric layer in OFETs. In addition, the biodegradability and nontoxicity of gelatin are well known, making it an ideal candidate for bioresorbable electronics [63]. It was reported that changing the amount of gelatin in the PVA–gelatin composite modulates the soluble properties of the films, resulting in optimized resolution of the layer during the fabrication of devices.

Significant insight into electronic materials can be gained from the items we recognize or handle daily. For example, Chang et al. [64] used pure albumen extracted from chicken egg white as a dielectric within OFETs. The surface smoothness, as measured by atomic force microscopy (AFM), had an RMS roughness of about 2 nm with outstanding dielectric properties, showing that albumen is applicable for OTFT applications. The image on the left in Fig. 4(c) [64] illustrates the configuration of the albumen-based device; it has a capacitance of about 10 nF·cm^{-2} and a dielectric constant, ε, of about 6, which are coherent with the dielectric constant of the denatured egg white, which is about 5.5 [65]. The output currents of these OTFTs were about 3×10^{-6} A, with negligible hysteresis and gate leakage currents of about 10^{-10} A. Furthermore, when this albumen-based dielectric layer was applied to a flexible OFET device, the inverter circuits showed modest electrical properties.

Aloe barbadensis Miller, commonly known as Aloe vera, is a juicy plant that grows in barren lands. Aloe vera gel is commonly and historically applied as an anti-inflammatory drug for the alleviation of insect bites and sunburn. The leaves contain a gel that is mostly water, with a small amount of glucomannans, amino acids, lipids, sterols, and vitamins [66]. The gel is economical, easy to handle, and applicable for biocompatible and biodegradable electronics. For these reasons, Aloe vera was considered for electronics development by Khor and Cheong [67], who studied the dielectric characteristics of common Aloe vera gel. A printed Aloe vera layer has an ε of about 4. Fig. 4(d) [68] shows a scheme of an n-type OTFT whose dielectric layer is based on a complex of Aloe vera paste derived from fresh leaves with SiO_2 nanoparticles, which enhanced the compatible properties of C_{60} with the Aloe vera gel. An analysis of the output properties was done directly after the fabrication of device and then again after 15 days, revealing decreased electrical properties, due to the hydration of the dielectrics with the oxidation of the semiconductor and electrodes [69]. Furthermore, a simple memory cell structure based on a dried Aloe vera film has been demonstrated, as shown in Fig. 4(d) [68]. The drying temperature of the films affected the physicochemical properties, causing variation of the device properties affecting the set and reset voltages. The switching property was highly reproducible, showing an I_{on}/I_{off} of about 1×10^4, a retention time of 12 h, and an endurance of 100 switching cycles.

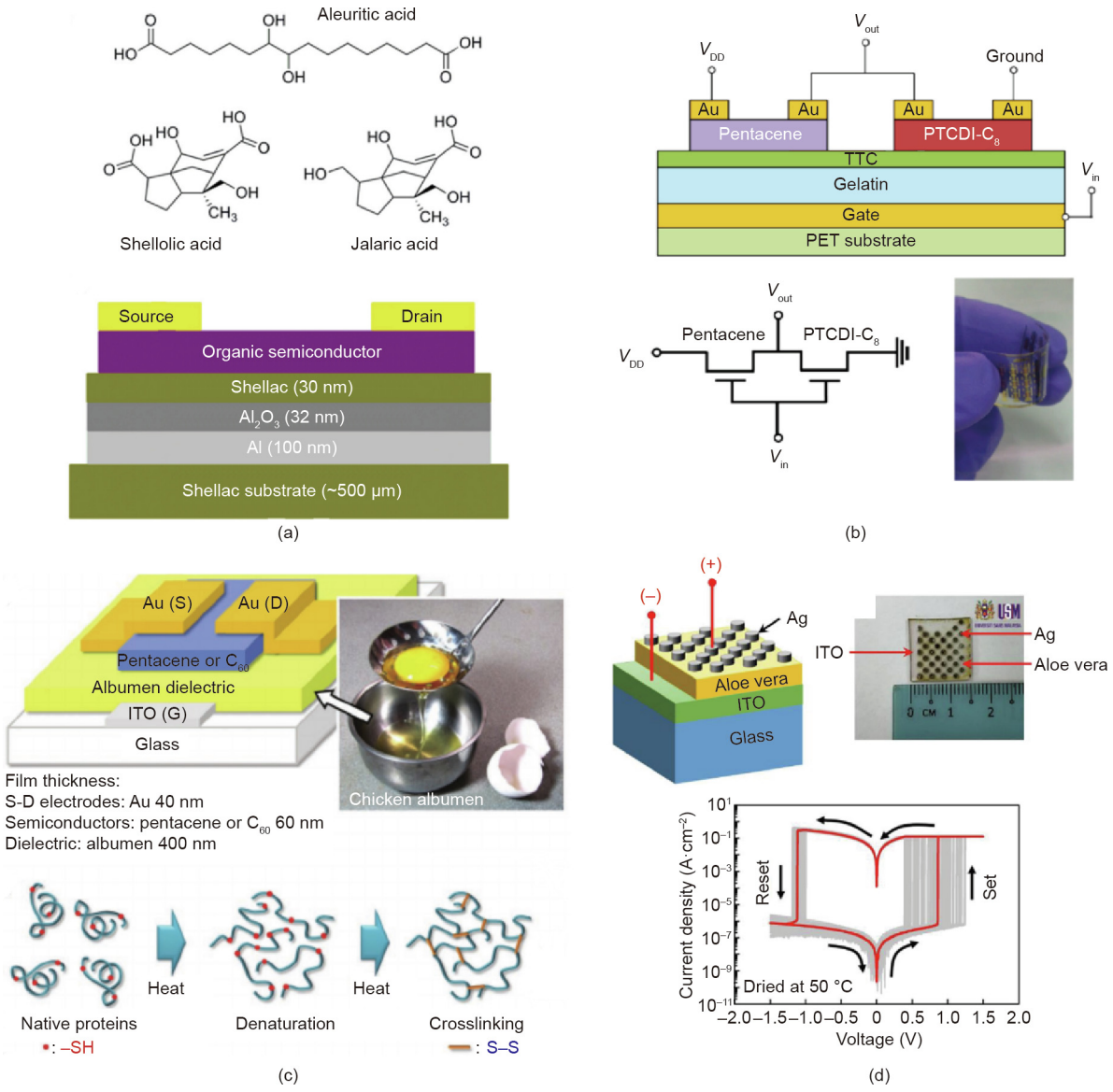

Fig. 4. Dielectric characteristics of resin, gelatin, albumen, and Aloe vera. (a) The fundamental chemical elements of shellac resin and schematic configuration of OTFT based on them; (b) a schematic illustration of an inverter device with gelatin as a gate dielectric layer, exhibiting flexibility; (c) a cross-linked albumen dielectric layer-based OTFT device; (d) a schematic configuration based on an Aloe vera memory device with electrical properties during resistance switching tests. TTC: tetratetracontane; PTCDI-C8: *N*,*N*′-Dioctyl-3,4,9,10-perylenedicarboximide. (a) Reproduced from Ref. [60] with permission of Royal Society of Chemistry, ©2013; (b) reproduced from Ref. [61] with permission of Elsevier, ©2010; (c) reproduced from Ref. [64] with permission of Wiley-VCH, ©2011; (d) reproduced from Ref. [68] with permission of Elsevier, ©2017.

2.2. DNA and nucleobases

DNA has attracted attention in academia and industry since its double-helix structure was first observed [70]. Beyond common biological applications of DNA material, its self-organizing mechanism has been of interest for nontraditional applications over the past couple of decades, including biological computing and information storage [71–74]. Engineers and scientists in the nanotechnology field have used DNA as a template to create sophisticated nanoscale or microscale structures [75–78]. Furthermore, long polymeric chains with a backbone exhibiting negative charges, which are similar to the initiation of molecular wire growth, have been used by researchers in the material and electrical sciences to explore charge transport characteristics at the atomic scale. More recent studies have investigated DNA's capabilities beyond the cell for feasible applications such as nanotechnology, information storage, electronic devices, biosensing, and so on. Enhanced convergence studies of diverse DNA-based research areas have led to the development of impressive and unique electronics that modulate signals with nanoscale accuracy. A typical intrinsic DNA material consists of two binding nucleotide chains with a width of only 2–3 nm but a length of several of base pairs. The double-helix configuration is based on the hydrogen bonding between pairs of nucleobases. A nucleotide comprises a pentose, a phosphate group, and a nitrogenous base (i.e., a nucleobase). Common DNA nucleobases include adenine (A), guanine (G), thymine (T), and cytosine (C). The energy levels of DNA-based material cover a wide range from the highest occupied molecular orbital (HOMO) to the lowest unoccupied molecular orbital (LUMO), which enables the selection of appropriate electrons and hole transport in electronics. As shown in Fig. 5(a) [79], electrodes such as indium–tin–oxide (ITO), Au, and poly(3,4-ethylenedioxythiophene) (PEDOT) with work functions of 4.7–5.1 eV are commonly applied to anodes to inject holes in opto-electronics. Al electrodes have a work function

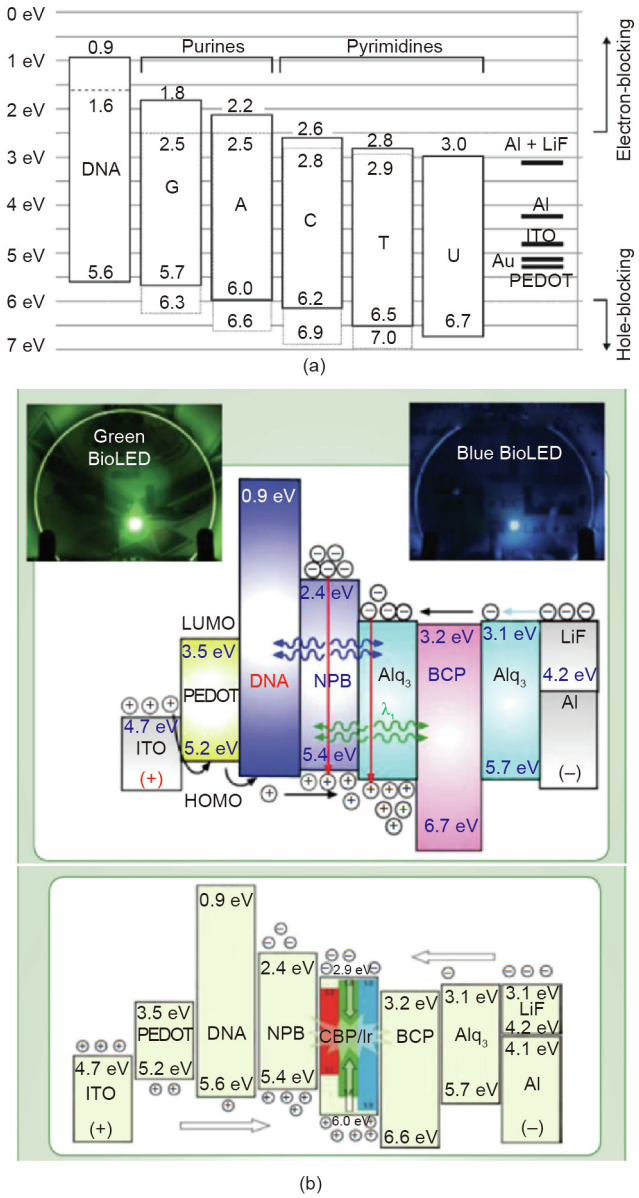

Fig. 5. DNA structure and its applications in organic light-emitting diodes (OLEDs). (a) The energy levels of DNA and nucleobases compared with electrodes; (b) fluorescent and phosphorescent OLEDs with a DNA-based electron-blocking and hole transport layer. NPB: *N*,*N*′-diphenyl-*N*,*N*′-bis(1-naphthyl)-1,1′-biphenyl-4,4″-diamine; Alq_3: tris(8-hydroxyquinolinato)aluminum; BCP: bathocuproine; CBP: 4,4′-bis(*N*-carbazolyl)-1,1′-biphenyl; Ir: iridium. (a) Reproduced from Ref. [79] with permission of Wiley-VCH, ©2015; (b) reproduced from Ref. [83] with permission of Optical Society of America, ©2011.

of 4.1–3.1 eV with a LiF layer, and are mostly applied as cathodes to inject electrons. Nucleobases have also been investigated for use in organic light-emitting diodes (OLEDs), due to their flexible control of charge transport. Steckl [80], Hagen et al. [81], and Lee et al. [82] demonstrated the application of DNA in OLEDs and highlighted the potential of DNA as a sustainable material that could be applied to optical waveguides and lasing components (Fig. 5(b) [83]). The use of DNA thin films incorporated with fluorescence-emitting components for OLEDs could also improve the brightness performance of the devices in comparison with conventional OLEDs, in which a thin DNA layer is applied as a high-efficiency electron-blocking layer (EBL) without interfering with the hole transport process. Accordingly, the DNA layer can generate excitons with fluorescent OLEDs decorated with specific fluorophores such as standard tris(8-hydroxyquinolinato)aluminum for green emission and *N*, *N*′-diphenyl-*N*,*N*′-bis(1-naphthyl)-1,1′-biphenyl-4,4″-diamine for blue emission, as shown in Fig. 5(b). When thin films of the DNA-surfactant complex are used in phosphorescent OLEDs, as demonstrated in Fig. 5(b), their brightness and efficiency are superior to those of their phosphorescent counterparts. In addition, Gomez et al. [84] demonstrated the use of T and A as the EBLs, which resulted in enhanced photoemission efficiency.

In subsequent studies, G, C, and uracil (U) were investigated as potential EBLs and hole-blocking layers (HBLs), including film fabrication and electronic characterization [84]. In that work, the nucleobases exhibited HOMO and LUMO energy levels comparable to those of DNA (i.e., ranging from 3.5 to 4.0 eV); furthermore, the electron affinity values, which ranged from 1.8 to 3.0 eV, were capable of increasing the number of combinations for the structure of the electronic device. Table 1 [79] outlines the optical characteristics of various nucleobases acting as EBLs and HBLs.

As shown in Fig. 5(a), the HOMO–LUMO energy level gaps of the nucleobases uniformly increase from 3.6 to 4.0 eV, corresponding to gray and black lines, respectively. The increase in the ionization potential HOMO follows this order: G < A < C < T < U. Therefore, G exhibits the minimum ionization potential, with a HOMO of about 6 eV and an electron affinity, LUMO, of about 2 eV; thus, it is an efficient hole acceptor that hinders electron transport. In contrast, U shows the greatest ionization potential of about 7 eV and an electron affinity of about 3 eV. Thus, it is an efficient electron acceptor that hinders hole transportation [85,86]. The results of previous studies [87–91] showed several variations because the researchers used individual measuring methods with discrete experimental situations; however, the common tendencies shown by the results were almost the same. With the addition of nucleobases, nucleic acids can be used for both hole and electron transport with blocking, and thus have potential for a wide range of applications. An early theoretical model suggested that DNA can be an effective conducting wire with sufficient delocalization of the charge transport along several nucleobase pairs [92]; in this case, the conduction is generally attributed to positive charges being moved along the chain by short-range processes [93,94]. The G nucleobase, which exhibits the highest HOMO energy level, is widely recognized as the dominant hole [95,96]. A simulation study of a G-dominant chain with Au electrodes (Fig. 6(a) [96]) demonstrated the high hole-hopping rate along the localized orbitals.

Although it is commonly suggested that the mechanism of charge transport follows the G bases, long-range charge transport is difficult to achieve, which results in saturation with conflicting or unreproducible results. The unique system of DNA also enables a variety of modifications to the material characteristics, including diameter, sequence, and rigidity, which can modulate the electrical characteristics. While examining the possibility of using DNA as electrical wires, G was determined to be the fundamental nucleobase due to its lowest oxidation potential compared with the other nucleobases (Figs. 6(b) [97] and (c) [98]). It can easily lose electrons under oxidative stress, which generates positive charges that go beyond the formed base and continue to move, following G-dominant sequences. Since G-dominant sequences decrease in oxidation potential, positive charges can transport from one G base to different G sequencing, attracting charge carriers [99]. Commonly, n- and p-type semiconductors employ electrons and holes to generate current, respectively. By considering this concept, the current can be modulated following the specific direction, which is a fundamental characteristic of semiconductor-based devices. (G + C)- and (A + T)-dominant sequences in the nucleobases exhibit p- and n-type characteristics, respectively [97,98]. Thus, it is theoretically possible to create base pairs of DNA with a short sequence for a logic element stronger than any silicon-based device, using

DNA's characteristics. Single-electron transistors based on DNA molecules have already been suggested [100].

As demonstrated by Zhang et al. [101], the use of DNA as capping layers enhanced charge injection in OTFTs, with an interlayer between the semiconductors and electrodes. As shown in Fig. 7(a) [101], the DNA layer aids the introduction of both holes and electrons. Here, the OTFTs were based on n-type semiconducting materials, (6,6)-phenyl-C_{70}-butyric acid methyl ester and 4,7-bis{2-[2,5-bis(2-ethylhexyl)-3-(5-hexyl-2,2′:5′,2″-terthiophene-5″-yl)-pyrrolo[3,4-c]pyr-rolo-1,4-dione-6-yl]-thiophene-5-yl}-2,1,3-benzothiadiazole, or diketopyrrolopyrrole (DPP)-containing small molecules. The charge-carrier mobility of the fabricated OTFTs with a DNA injection layer exhibited an improved charge of up to one order compared with devices without an interlayer (Fig. 7(b) [101]). As the interlayer role of n-type and ambipolar semiconductors, top-contact OTFTs incorporate the DNA layer by spray coating, which acts as a hole injection layer [102]. By introducing a DNA layer to OTFTs, the drain current at the saturation region increased from about 0.6 to 1.5 μA, which corresponds to an increase in charge carrier from about 0.01 to 0.1 $cm^2 \cdot V^{-1} \cdot s^{-1}$. This improvement in device performance was derived overall from the decrease in contact resistance induced by dipole formation between the electrodes and the semiconductor interface, by which the hole injection barrier decreased.

Furthermore, since the 1940s, the LC phases in hydration have been demonstrated, making an important contribution to the measurement of X-ray structural factors free from complications of DNA chain sequences and interchain correlation [103,104]. Subsequently, a structure analysis of duplex B-form DNA exhibiting LC phases in the solution state was performed using optical [105–108], X-ray [109], and magnetic resonance [110,111] measurement techniques with respect to chain length from mega-base pairs (bp) to roughly 100 bp, corresponding to semiflexible polymers and rigid rod-like elements, respectively. This is a similar size to the B-form of DNA, which shows a bend persistence length, L_p, of about 45 nm [112]. The analysis confirmed the isotropic phase (Iso), chiral nematic (N^*), uniaxial columnar (C_U), and higher-ordered columnar (C_2) LC phases, as well as the crystal (Cr) phases, depending on DNA concentration. By allowing the LC properties of DNA to align the host materials, as CNCs have done [113–115], we demonstrated OTFTs based on highly ordered and oriented complexes of the π-conjugated polymer, poly[3-(potassium-7-hexanoate)-thiophene-2,5-diyl] (P3PHT), with a self-assembled DNA template (Fig. 7(c)) [116]. The addition of DNA induced highly ordered P3PHT aggregates, whose nucleation generated the growth of P3PHT aggregate, while residual P3PHT underwent spontaneous nucleation. AFM with polarized optical microscopy analysis confirmed that the DNA template induced the molecular orientation of the P3PHT guest. The anisotropic complexes based on host materials exhibited anisotropic electrical and optical properties depending on the interchain (π–π stacking) and intrachain transport (π-conjugation). The films of the P3PHT/DNA complex exhibited somewhat vertical separation, in which the interface between the source/drain electrodes and the semiconducting layer was mainly present with DNA, ensuring the lower barrier of hole injection, similar to previous studies [101]. Furthermore, the distinct chemical and physical cooperation with the electrostatic binding attraction between DNA and Cu^{2+} allowed p-doping, giving the device a mobility of about 0.2 $cm^2 \cdot V^{-1} \cdot s^{-1}$.

As mentioned above, the length of a DNA chain inspired early studies of charge transport along a DNA chain, considering DNA as a nanowire [117]. Studies have also examined the improvement of luminophore optical emission based on intercalation in the double-helix DNA host [118], which enabled research into organic electronic applications using DNA. Although there have been attempts to facilitate natural DNA salts for thin-film electronics, it is difficult to fabricate uniform films from an aqueous solution [119]. For this reason, cationic surfactants (e.g., cetyltrimethylammonium chloride) were incorporated with the negatively charged DNA backbones, generating the DNA-surfactant salt DNA-cetyltrimethylammonium (CTMA) (Fig. 8(a)) [119]. The intercalated chains could then be dissolved in alcohol solvents, which can be used in the spin-coating process [120] in which the optical, electrical, and magnetic measurements of the thin films of DNA-CTMA have been done [121]. The DNA-CTMA complex is well known for its energy levels, and makes an excellent EBL with a hole transport layer for organic electronics (Fig. 8(b) [122]). In capacitor and gate dielectric applications, it has a high dielectric constant, *K*, of about 8 under low frequencies; in complex cases involving ceramics, the dielectric constant can be as high as 15, and disruption of the dielectric property of 4 $MV \cdot cm^{-1}$ has been reported in the case of a sol–gel mixture [123,124]. Therefore, DNA films are commonly used as gate dielectric layers, in which OTFTs based on DNA-CTMA and Al_2O_3 gate dielectric complexes have demonstrated reduced hysteresis compared with pristine DNA-CTMA-based OTFTs (Fig. 8(c)) [122]. In addition, modified DNA with photoreactive side-chains has demonstrated cross-linking properties via ultraviolet (UV) irradiation, resulting in different solubility and dielectric characteristics with improved hysteresis properties [122,125,126]. A DNA-based complex with high dielectric-

Table 1
Summarized results for DNA-based EBLs and HBLs [79].

Type	Turn-on (V)	Maximum luminance ($cd \cdot m^{-2}$)	Maximum current efficacy ($cd \cdot A^{-1}$)	Maximum luminous efficacy ($lm \cdot W^{-1}$)	Quantum efficiency (%)	
					External	Internal
EBL type						
Baseline	3.25	95.179	38.5	22.3	10.7	59.4
G	4.75	17.191	44.3	21.9	12.3	68.3
A	5.00	82.289	51.8	21.2	14.3	79.4
C	5.00	5.646	36.1	14.5	10.0	55.6
T	7.75	3.844	22.6	6.9	6.3	35.0
U	7.00	21.000	3.3	1.2	0.9	5.0
DNA-CTMA	3.75	60.061	43.3	25.6	12.0	66.7
HBL type						
G	6.00	16.000	1.3	0.6	0.4	2.2
A	5.50	215.000	10.0	0.4	0.3	1.6
C	5.50	217.000	5.2	2.1	1.5	8.3
T	5.50	362.000	15.1	5.0	4.2	23.3
U	4.25	4.045	16.3	7.4	4.6	25.6

CTMA: cetyltrimethylammonium.

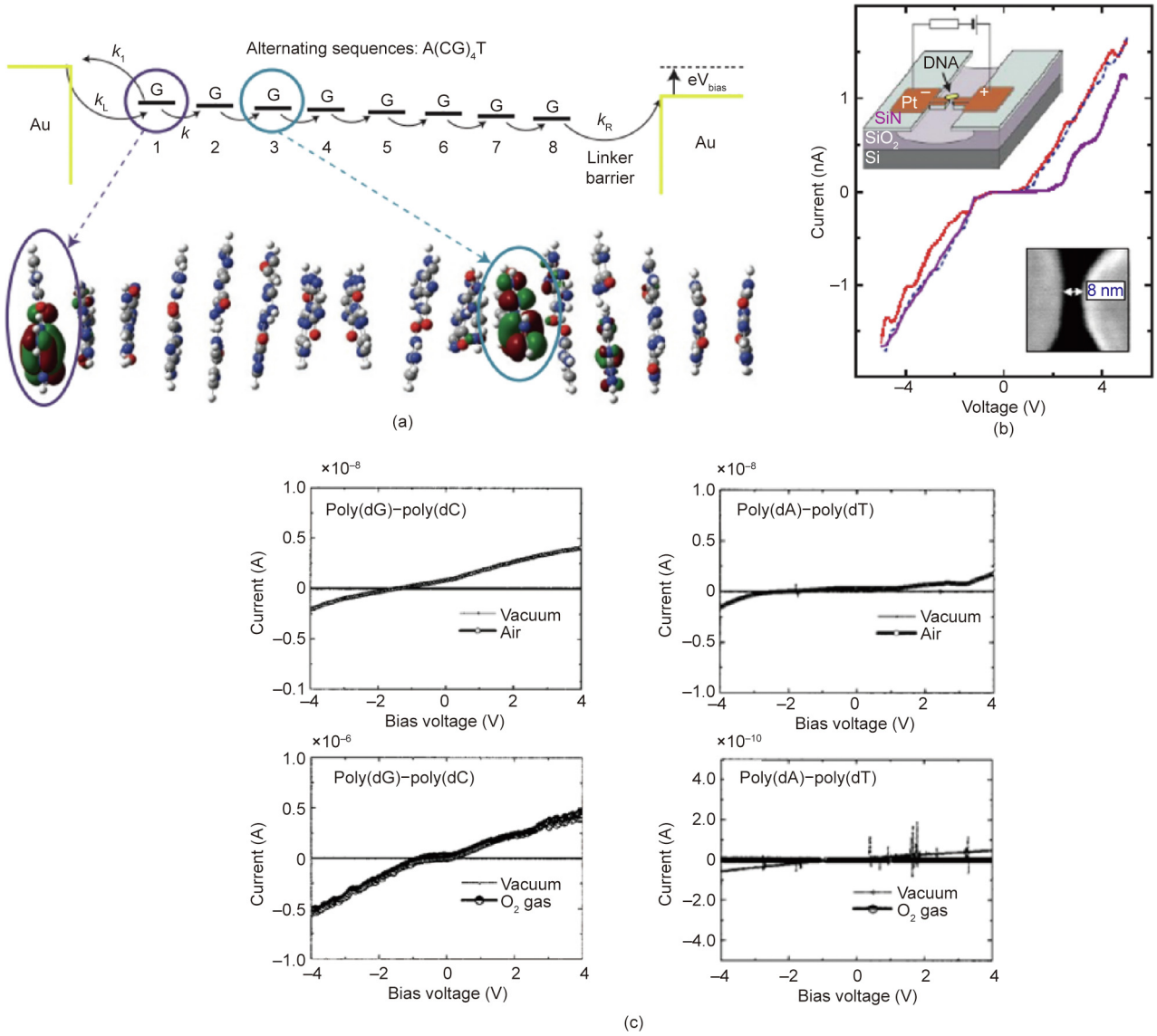

Fig. 6. Charge-carrier hopping along DNA. (a) Hole hopping following the G bases in DNA cooperated between Au electrodes; (b) electrical properties of a double-stranded poly(G)–poly(C) DNA molecule trapped between electrodes; (c) current–voltage curves of poly(dG)–poly(dC) and poly(dA)–poly(dT) DNA films under air and oxygen conditions. k_L,k_1, k_R, and k are the hole transfer rate constants from the left electrode to the first G of the DNA, from the first G back to the left electrode, from the last G of the DNA to the right electrode, and between adjacent hopping sites, respectively. eV_{bias}: electron voltage of bias. (a) Reproduced from Ref. [96] with permission of Springer Nature, ©2015; (b) reproduced from Ref. [97] with permission of Springer Nature, ©2000; (c) reproduced from Ref. [98] with permission of AIP Publishing, ©2002.

constant ceramics, such as $BaTiO_3$ and TiO_2, has been reported, which would further improve the electrical properties of organic electronic devices [123].

2.3. Semiconductors

A number of π-conjugated molecules, which have intrinsic semiconducting properties and can be applied in the active components of optics and electronics, are present in nature. For example, the molecules related to photosynthesis, such as porphyrins and polyenes, are chromophores with delocalized conjugation whose chemical structures are very similar to those of synthetic conjugated polymers. Furthermore, organic dyes with π-conjugation have been shown to be harmless and can be used in textiles, inks, and more. In 1975, Tang and Albrecht [127] produced a sandwiched photovoltaic diode based on a chlorophyll a thin film. This is a typical example of utilizing naturally available semiconductors for organic electronics. However, there have been critical problems in the practical application of such materials, including low power-conversion efficiency and low charge transport with unstable operation.

Research by Wang et al. [128] on the natural carotenoids, including lycopene, β-carotene, and fucoxanthin, demonstrated their electron-donor property when integrated with an electron-acceptor, (6,6)-phenyl-C_{61}-butyric acid methyl ester (PCBM), in OPVs (Fig. 9(a)). Compared with amorphous films such as fucoxanthin and β-carotene, lycopene films can easily be made using a spin-coating process, which generates high-performance OPVs. The electrical characteristics and external quantum efficiency graphs showed the following performance ranking: lycopene, β-carotene, and fucoxanthin. However, an operational problem remains: rapid oxidation under an oxygen-based environment, such as ambient conditions, although the metabolism in the biological system continually regenerates the molecules [129].

Most organic dyes and pigments have intramolecular and intermolecular hydrogen bonding, which are correlated with the

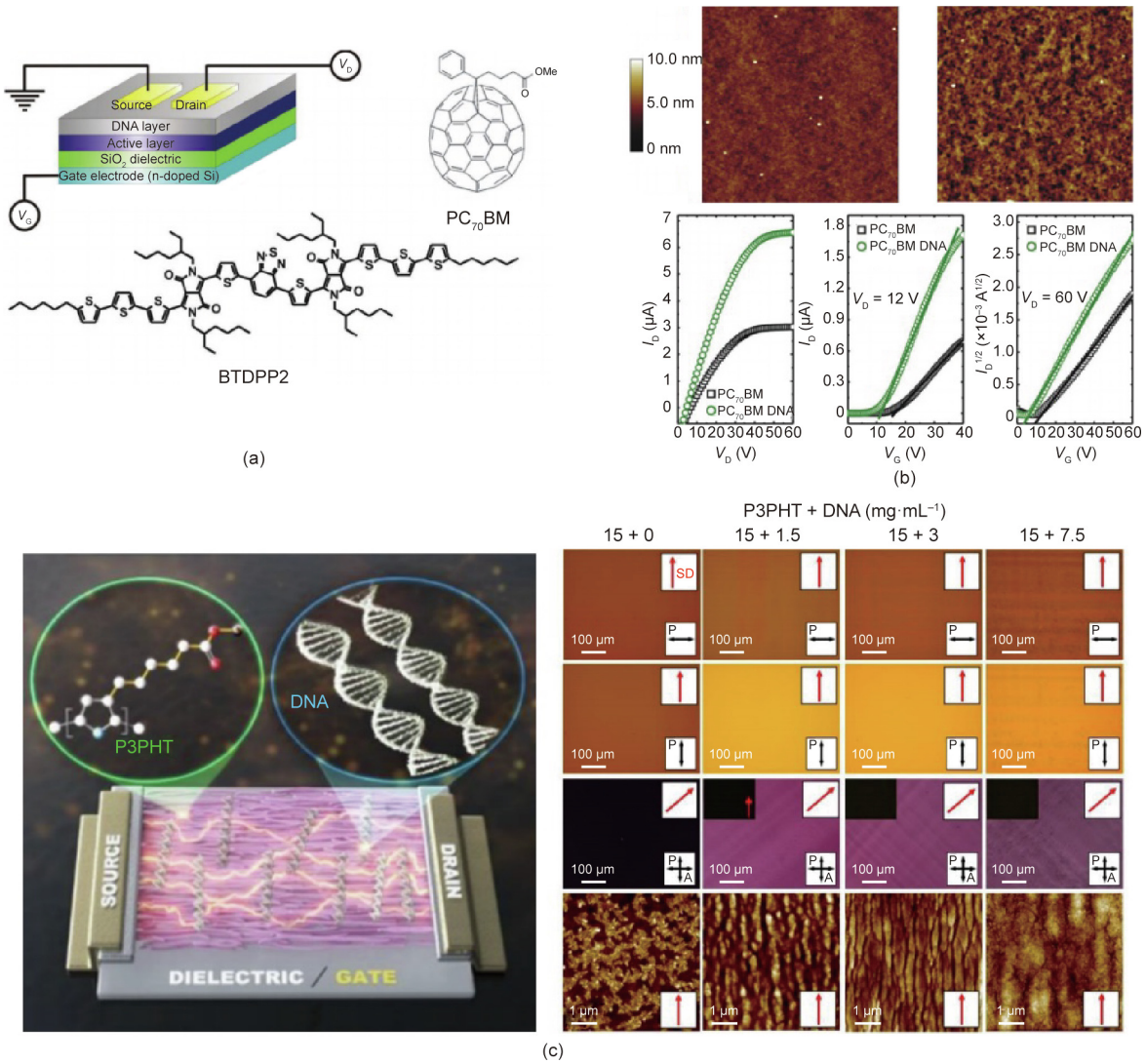

Fig. 7. Interlayer characteristic of DNA between organic semiconductors and electrodes. (a) Schematic illustration of the n-type and ambipolar OTFT configuration based on charge injection through DNA; (b) topography measurement and electrical characterization of OFETs depending on DNA interlayers; (c) with its versatile properties, DNA can function as a template for a semiconducting polymer and interlayer in OTFT. $PC_{70}BM$: (6,6)-phenyl-C70-butyric acid methyl ester; BTDPP2: 4,7-bis{2-[2,5-bis(2-ethylhexyl)-3-(5-hexyl-2,2′:5′,2″-terthiophene-5″-yl)-pyrrolo[3,4-c]pyr-rolo-1,4-dione-6-yl]-thiophene-5-yl}-2,1,3-benzothiadiazole; P3PHT: poly[3-(potassium-7-hexanoate)-thiophene-2,5-diyl]; SD: shearing direction; P: polarizer; A: analyzer; V_D: drain voltage; V_G: gate voltage; I_D: drain current. (a), (b) Reproduced from Ref. [101] with permission of Wiley-VCH, ©2012; (c) reproduced from Ref. [116] with permission of the American Chemical Society, ©2020.

stability of the desirable color properties. For example, organic dyes and pigments that become colorless in a dissolved solution contain a fused-ring configuration based on carbonyls or amines [130–132]. The hydrogen bonding induces aggregation and crystallization, resulting in bathochromic shifts in the wavelength of light absorption. Therefore, intrinsically stable small molecules can aggregate into crystal forms, exhibiting high UV–visible absorption and stability resulting from the high energy of the crystal lattice. Among such molecules, indigo derivatives derived from plants and animals are the most well-known natural dyes in history (Fig. 9(b)) [133]. It is notable that a chemical reduction process is necessary to obtain water-soluble leucoindigo forms, as indigo is insoluble in a neutral state due to its high crystal lattice energy. In what is known as the vat dyeing process, leucoindigo permeates into the fiber being dyed; next, oxygen oxidizes the leucoindigo and pulls it back into the air, resulting in permanent coloring of the fabric. This is a nontoxic process based on the versatile and reversible redox states of the molecules, and is used extensively in the industrial dyeing of 20 000 t of blue denim fabric per year.

Thin indigo films for organic electronics can be fabricated via vacuum sublimation at temperatures below 300 °C, since the indigo can be finely cleaned using a sublimation technique, although the inherent ionic content of the coated films is not desirable. Irimia-Vladu et al. [134] studied ambipolar semiconducting properties with comparable electron and hole mobilities of about 0.01 $cm^2 \cdot V^{-1} \cdot s^{-1}$ and excellent stability.

The natural pigment Tyrian purple, 6,6′-dibromoindigo, which was historically derived from sea snails (Fig. 10), exhibits ambipolar semiconducting properties and has potential for application in heterojunction diodes at the near-infrared wavelength region [135,136]. The van der Waals forces between the bromine atoms enhance their molecular packing, with balanced charge-carrier mobilities of approximately 0.5 $cm^2 \cdot V^{-1} \cdot s^{-1}$ (Fig. 10(a)) [137]. Due to the crystal structure, the intermolecular hydrogen bonds can be oriented into hydrogen-bonded chains, in which the molecular stacking direction is vertical to the hydrogen-bonding direction. Various studies have shown that the orientation of crystal growth has a strong effect on the holes and electron transport

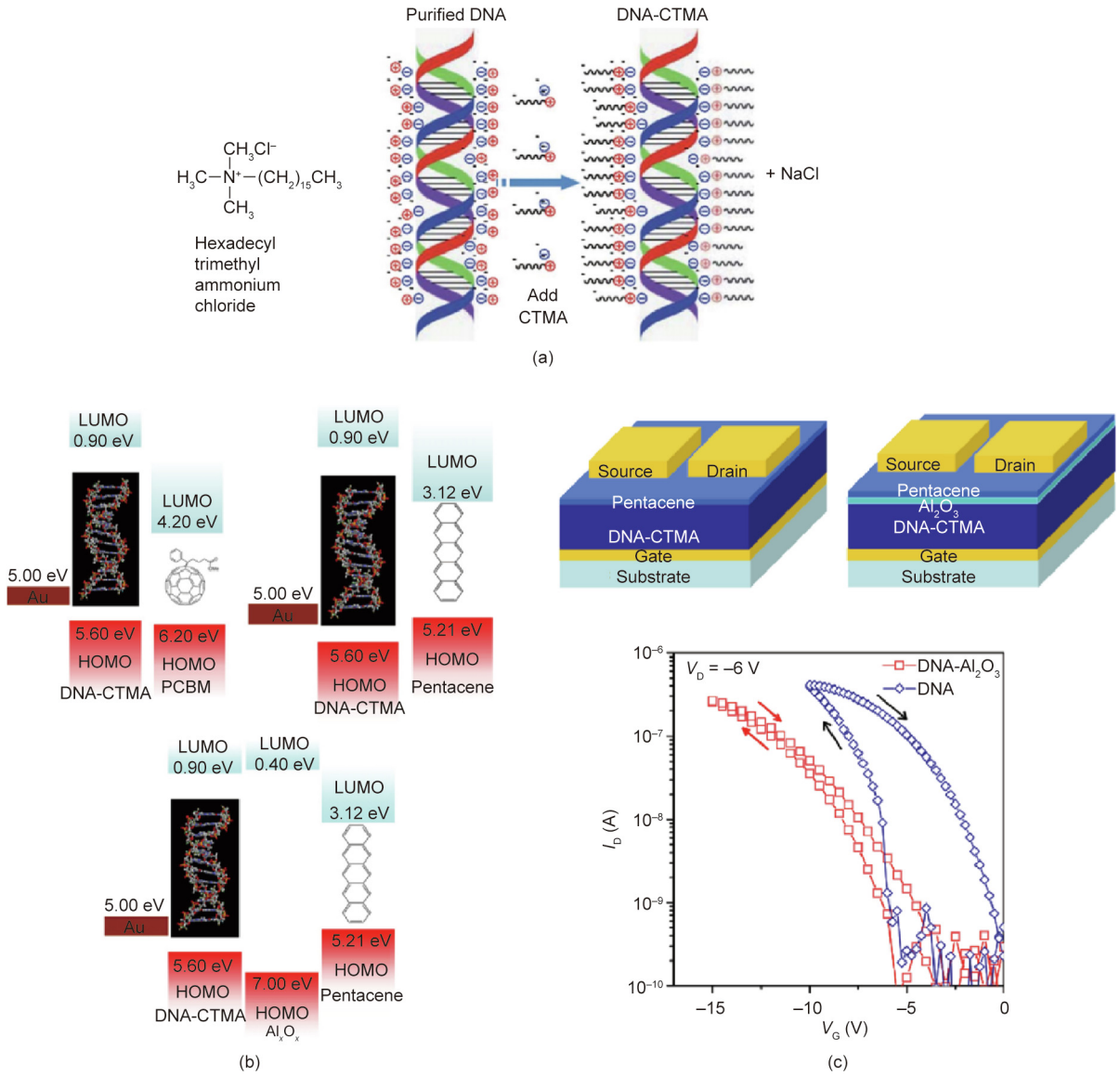

Fig. 8. The DNA-CTMA complex for OTFT. (a) The chemical configuration of CTMA: hexadecyl trimethylammonium chloride, with an illustration of how surfactants interact with DNA; (b) energy levels of DNA-CTMA compared with those of a Au electrode, pentacene, and (6,6)-phenyl-C_{61}-butyric acid methyl ester (PCBM) with Al_2O_3; (c) schematic of DNA-CTMA OTFTs and their transfer and output curves. (a), (b) Reproduced from Ref. [119] with permission of the Royal Society of Chemistry, ©2014; (c) reproduced from Ref. [124] with permission of Elsevier, ©2007.

[138,139]. Some chemically modified indigo derivatives have also been applied to organic electronics [140,141]; the derivatives showed different molecular packing and crystallization depending on the substrates and deposition conditions. The introduction of hydrogen-bonding groups increases stability and aggregation control, making it possible to guarantee the desired color for the industrial organic industry [142]. Some pigments, which have been investigated for toxicity and environmental effects, can be utilized in a large range of customer commodities, including paints, inks, diverse cosmetics, and tattoos [143]. An example of a well-known synthesized hydrogen-bonding dye is quinacridone [144], which has been studied for use as an active layer in OPV and OTFTs; it exhibits hole mobilities of 0.1 $cm^2 \cdot V^{-1} \cdot s^{-1}$ with an electron mobility approximately one order of magnitude lower [145]. Moreover, quinacridone exhibits stable device properties under ambient conditions without an encapsulation layer. Epindolidione is another structural isomer of indigo based on hydrogen bonding. Unlike quinacridone, epindolidione can be prepared by solid phase rearrangement at high temperatures with vacuum conditions [146]. In addition, epindolidione exhibits ambipolar electrical properties like its isomer indigo, and has a higher hole mobility of about 0.8 $cm^2 \cdot V^{-1} \cdot s^{-1}$ [147]. Quinacridone and epindolidione show luminescence in a solution and in a solid condition; however, indigo does not exhibit luminescence because fast proton transfer occurs in light, resulting in efficient nonradiative deactivation at the excited state (Fig. 10(b) [148]). Epindolidione and quinacridone demonstrate many excimer-based luminescence behaviors in the solid state, derived from intermolecular hydrogen-bonding interaction with efficient delocalization of excited states between adjacent molecules [148]. Table 2 [33,51,56,58,60] summarizes the OFETs electrical characterization of different examples of indigo derivatives presented in previous studies.

2.4. Conductors

Biocompatible and biomaterial-originating conductive materials, including ionic conductors, have been studied recently in different medical devices. The first organic electronic device related

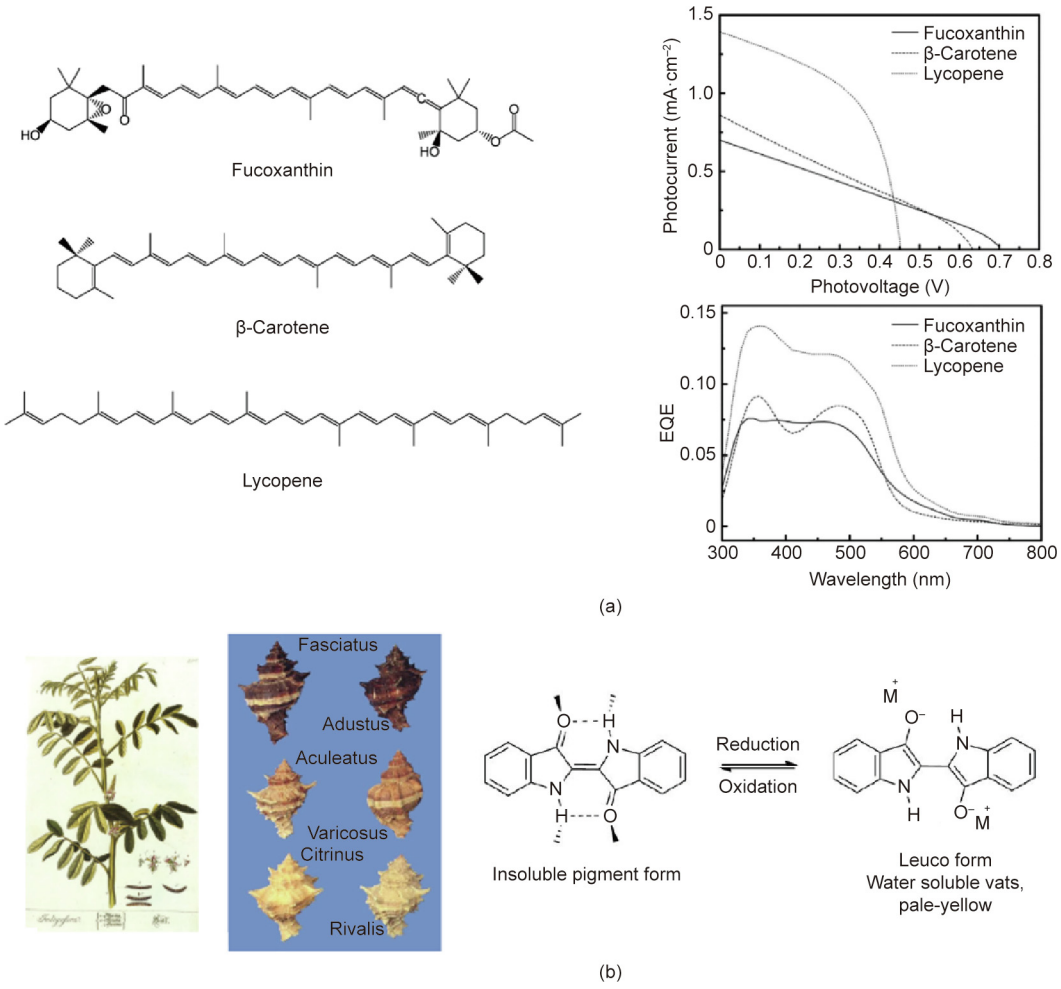

Fig. 9. Examples of bio-origin semiconductors. (a) Molecular structure of carotenoids derivatives with representative output curves of bixin; (b) image of *Indigofera tinctorial*, a typical origin of indigo, and diverse snails from the Thaisidae and Muricidae families, the origin of Tyrian purple dyes made via vat dyeing chemistry. EQE: external quantum efficiency. (a) Reproduced from Ref. [128] with permission of the American Chemical Society, ©2013; (b) reproduced from Ref. [133] with permission of Wiley-VCH, ©2013.

to such materials was based on eumelanin [149], a brown and black pigmentation material derived from animals, including humans, the electrical conductivity of which depends strongly on hydration. Based on the earliest report on the conductivity of melanin, eumelanin was applied to diverse diodes in a sandwich configuration [150,151]. Recently, it has been suggested that a thin-film conductor for biomedical applications can be fabricated with biological tissue and bio-absorbability [152]. For charge transport mechanisms along eumelanin, proton conductivity is more appropriate than the amorphous semiconductor model (Fig. 11(a)) [153]. Eumelanin demonstrated hysteresis properties within an Au/eumelanin/ITO/glass configuration at a specific voltage at different voltage sweep speeds, such as 1, 9, and 12 $mV{\cdot}s^{-1}$, which was performed under ambient conditions (Fig. 11(a-I)). Hysteresis was exhibited in a vacuum environment with dark and light irradiation, with a sweep rate of 9 $mV{\cdot}s^{-1}$ (Fig. 11(a-II)). Here, negligible hysteresis is present in the current graphs, even under white light illumination. Comparable hysteresis properties have appeared in various conjugated polymer systems [154].

Therefore, proton conductors have been widely studied in fuel cell applications, and their great potential for biocompatible electronics has recently been recognized. There are two focuses for this research interest. First, naturally derived proton conductors can be applied to sustainable devices. Second, many biological pathways contain protons, so the proton–electron interface is interesting in terms of biomedical devices. As many conductive polymers can transport both ions and electrons, they are uniquely suitable for bioelectronics interface materials. This is not feasible for conventional metal-based conductors. In a recent study [155], conductive polysaccharide-based transistors were tuned by the electric field effect of the gate, in a practical demonstration of the electron–proton interface. An outline of the device is shown in Fig. 11(b) [155]. The apparatus utilizes a chitosan polymer extracted from chitin by deacetylation, which comprises the exoskeleton. Chitosan is commonly derived from shrimp. Practical applications of bio-origin conductors are still limited, but the branch of synthetic conductive polymers is comparatively saturated. For example, polyaniline, poly(pyrrole), and poly(thiophene) exhibit outstanding biocompatible properties for biomedical applications [156–160].

Most importantly, a PEDOT system doped with polyanionic poly (styrene sulfonate) (PEDOT:PSS) has been used in various sensor applications with *in vivo* demonstrations. A report on cell proliferation in PEDOT:PSS films suggested that there was no toxicity. PEDOT:PSS is also applicable as polymer electrodes in biological brain tissue for bioelectric corticography, and exhibits an excellent signal-to-noise ratio compared with typical measurements [161]. An interface conductive PEDOT nanotube also succeeded in neural recording [162]. PEDOT can also be electropolymerized in living brain sites, achieving therapeutic effects (Fig. 11(c)) [163,164]. By polymerizing PEDOT directly in brain tissue, a conductive network

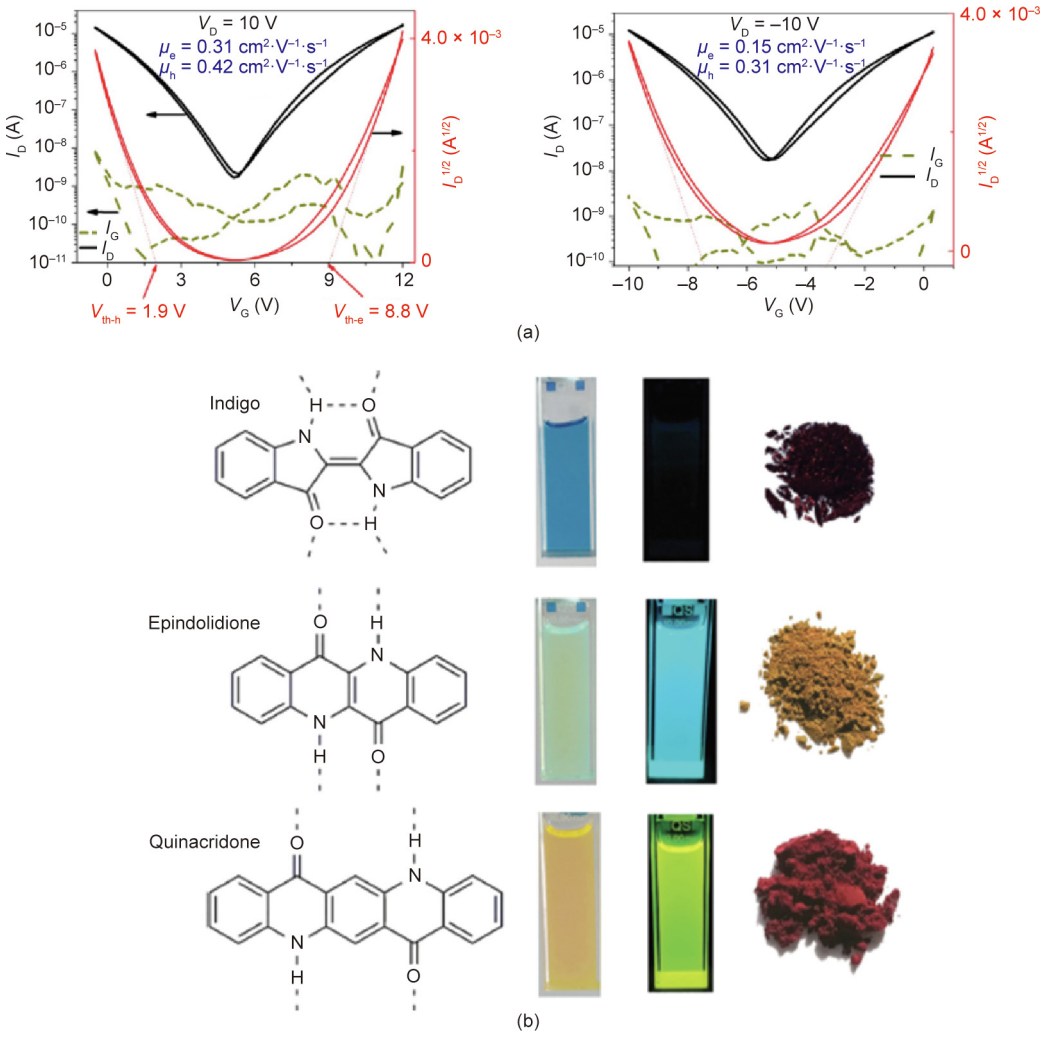

Fig. 10. Tyrian purple-based OTFT devices and the luminescence properties of indigo derivatives. (a) Ambipolar semiconducting properties of Tyrian purple with transfer curves; (b) varying luminescence quantum yields of powder and solution state depending on the molecular structures of indigo derivatives. μ_e: electron mobility; μ_h: hole mobility; V_{th-e}: threshold voltage for electron; V_{th-h}: threshold voltage for hole. (a) Reproduced from Ref. [137] with permission of Elsevier, ©2012; (b) reproduced from Ref. [144] with permission of Wiley-VCH, ©2015.

Table 2
Electrical characteristics of indigo and its derivatives.

Name	HOMO (eV)	LUMO (eV)	E_g (eV)	μ_e (cm^2·V^{-1}·s^{-1})	μ_h (cm^2·V^{-1}·s^{-1})	References
Indigo	−5.5	−3.8	1.7	1.0×10^{-2}	1.0×10^{-2}	[51]
Tyrian purple	−5.8	−4.0	1.8	0.4	0.4	[56,58]
Cibalackrot	−5.6	−3.5	2.1	9.0×10^{-3}	5.0×10^{-3}	[33]
Thioindigo	—	—	1.9	1.0×10^{-4}	6.0×10^{-4}	[51]
Epindolidion	−5.6	−2.9	2.7	—	1.5	[60]

E_g: bandgap energy.

is formed that controls the tissue and enables unique intimate and sensitive contact between the electrodes and the plasma film of the nerve cell. The large surface area of the PEDOT networks facilitates signal transmission between ion conductive tissue and electron conductive devices, and transmits electronic charges outside the tissue.

In addition, PEDOT has been used for efficient anion conductors, and PSS functions as a conductive path for cations including Ca^{2+}, Na^+, and K^+ [165,166], and even for the neurotransmitter acetylcholine [167,168]. In addition, the electro-polymerization of PEDOT thin films was achieved based on aqueous microemulsion (Fig. 11(c)), which affords different functionalization, such as ethylenedioxythiophene (EDOT)–OH, C_2–EDOT-COOH, C_4–EDOT–COOH, C_2–EDOT–NHS, and EDOT–N_3, resulting in tunable bio-interfaces. The diverse surface configuration was demonstrated successfully by surface templates with little inherent cytotoxicity and low inflammatory reaction during implantation, which can be applied to biosensing and bioengineering applications. Fig. 11(d) [167] provides a demonstration of a voltage pump based on PEDOT-derived acetylcholine. PEDOT:PSS preparations function as ion electronic interface materials for converting ion currents to and from electronics [156,169]. The feasibility of the side

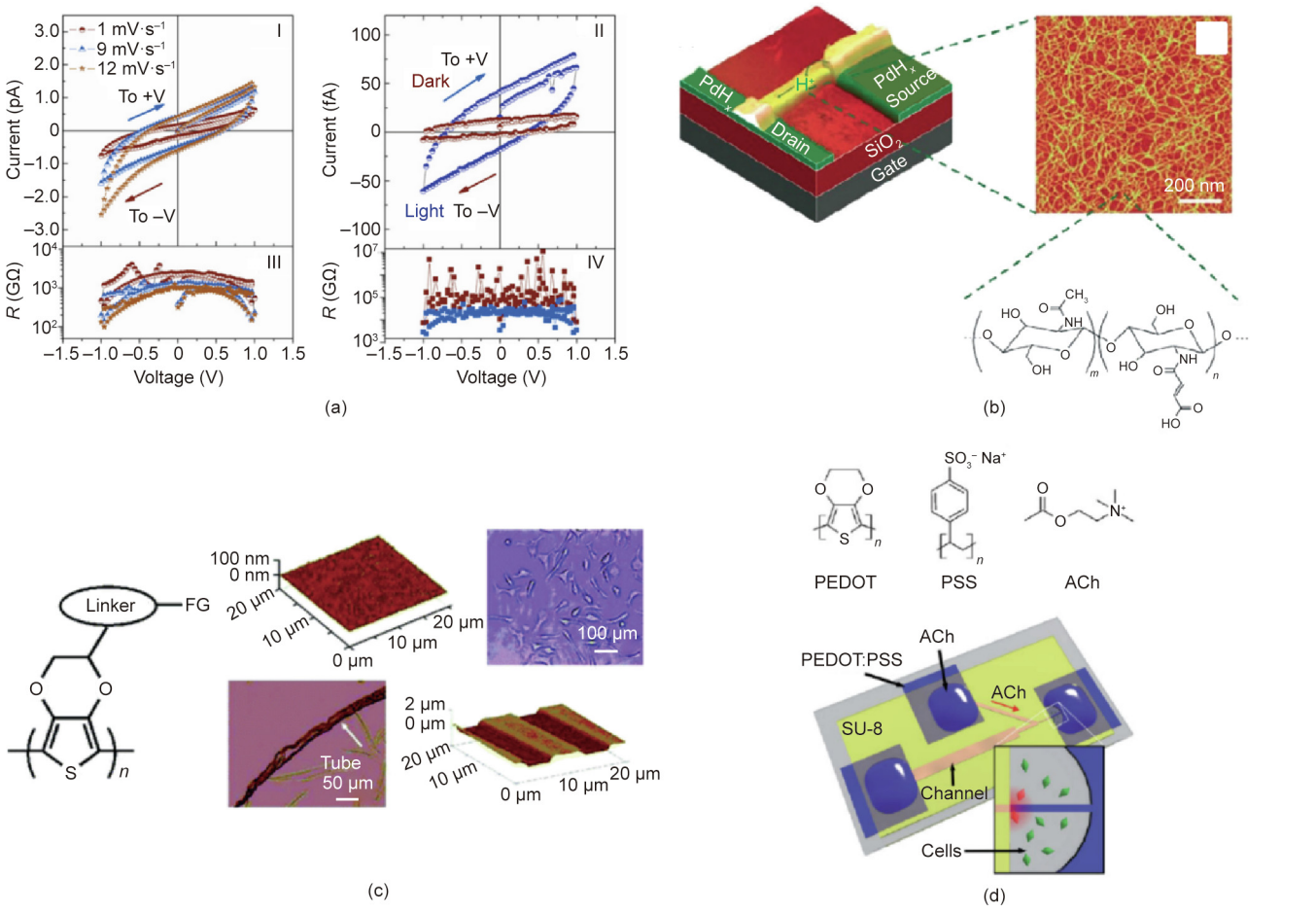

Fig. 11. Sustainable conductor applications. (a) Hysteresis test of the Au/eumelanin/ITO/glass configuration with a diverse voltage sweep rate and light exposure; (b) a bioprotonic transistor based on chitosan modulating the protonic charge; (c) therapeutic effects of PEDOT polymerized in living cells on an electrode substrate; (d) a PEDOT-based organic electronic ion pump made using microfabrication techniques for substance delivery. R: resistance; FG: functionalized group; ACh: acetylcholine. (a) Reproduced from Ref. [153] with permission of Elsevier, ©2010; (b) reproduced from Ref. [155] with permission of Springer Nature, ©2011; (c) reproduced from Ref. [164] with permission of the American Chemical Society, ©2008; (d) reproduced from Ref. [167] with permission of Wiley-VCH, ©2009.

transportation of about 150 Da of biomolecules with positive charges has been demonstrated; prepared circuits based on 10 μm channels allowed accurate material delivery, such as exact concentrations within the millimole scale. An organic electronic ion pump device exhibited direct connection of electronic properties, such as current and voltage, with the related delivery rate. Furthermore, numerous other conductive polymers, including polyaniline and polypyrrole, have been confirmed to be nontoxic [170]. Both polymers are biocompatible and do not trigger a response in the immune system, while maintaining good mechanical properties, such as flexibility, in biological systems. Although these common conductive polymers have been shown to be harmless and highly biologically compatible, further research into their biodegradation within an active biosystem is needed.

3. Conclusions and perspectives

In this study, we reviewed the use of ecofriendly materials in opto-electronics and discussed their promising—and practical—electronic performance as a replacement for conventional inorganic or fossil-fuel-based materials. Materials originating from nature can be used as passive or active components in electronic devices, in applications such as substrates, templates, insulators, semiconductors, and conductors. However, issues remain with their direct application as active electronic components in sustainable electronics, limiting their effective integration with opto-electronic devices. First, solubility is of concern because eco-friendly materials will only dissolve in water-based solvents, which can be harmful to device fabrication. Second, thermal stability should be considered due to the numerous hydroxyl groups in natural materials, which would suffer under the high temperatures required for device fabrication, deteriorating the stability of both the device elements and device performance. The third issue to consider is tuning the degeneration rate of sustainable materials integrated with common inorganic or fossil-fuel-based materials, as some materials can be vulnerable to device preservation issues. Despite these issues, sustainable materials continue to draw global attention for the vast number of options they open up and for their ecofriendly properties. In addition, there is room for improvement in the electrical properties and stability of such materials by means of physical and chemical modifications and composite technologies. There are abundant opportunities for further investigation, ranging from the verification of sufficient balanced bio-origin materials that are applicable for device configuration and advancement through optimization, to commercialized prototypes. Ultimately, from natural materials to electronic devices, this area of investigation provides insight into the merging of a wide range

of multidisciplinary sciences, such as chemical engineering, material science, biotechnology, and electronic engineering, in order to advance the next generation of sustainable devices.

Acknowledgements

This work was supported by a grant from the National Research Foundation (NRF) funded by the Korean Government (MSIT, 2017R1E1A1A01072798 and 2019K1A3A1A14065772).

Compliance with ethics guidelines

Moon Jong Han and Dong Ki Yoon declare that they have no conflict of interest or financial conflicts to disclose.

References

[1] Bettinger CJ, Bao Z. Biomaterials-based organic electronic devices. Polym Int 2010;59(5):563–7.
[2] Kim DH, Lu N, Ma R, Kim YS, Kim RH, Wang S, et al. Epidermal electronics. Science 2011;333(6044):838–43.
[3] Kim YJ, Chun SE, Whitacre J, Bettinger CJ. Self-deployable current sources fabricated from edible materials. J Mater Chem B Mater Biol Med 2013;1(31):3781–8.
[4] Norton JJS, Lee DS, Lee JW, Lee W, Kwon O, Won P, et al. Soft, curved electrode systems capable of integration on the auricle as a persistent brain–computer interface. Proc Natl Acad Sci USA 2015;112(13):3920–5.
[5] Tao H, Hwang SW, Marelli B, An B, Moreau JE, Yang M, et al. Silk-based resorbable electronic devices for remotely controlled therapy and *in vivo* infection abatement. Proc Natl Acad Sci USA 2014;111(49):17385–9.
[6] Balde K, Wang F, Huisman J, Kuehr R. The global e-waste monitor 2014: quantities, flows and resources. Bonn: United Nations University; 2015.
[7] Jambeck JR, Geyer R, Wilcox C, Siegler TR, Perryman M, Andrady A, et al. Marine pollution. Plastic waste inputs from land into the ocean. Science 2015;347(6223):768–71.
[8] Shah AA, Hasan F, Hameed A, Ahmed S. Biological degradation of plastics: a comprehensive review. Biotechnol Adv 2008;26(3):246–65.
[9] Singh B, Sharma N. Mechanistic implications of plastic degradation. Polym Degrad Stabil 2008;93(3):561–84.
[10] Kang SK, Murphy RKJ, Hwang SW, Lee SM, Harburg DV, Krueger NA, et al. Bioresorbable silicon electronic sensors for the brain. Nature 2016;530(7588):71–6.
[11] Li J, He Y, Inoue Y. Study on thermal and mechanical properties of biodegradable blends of poly(ε-caprolactone) and lignin. Polym J 2001;33(4):336–43.
[12] Hosoda N, Tsujimoto T, Uyama H. Plant oil-based green composite using porous poly(3-hydroxybutyrate). Polym J 2014;46(5):301–6.
[13] Nigam PS, Singh A. Production of liquid biofuels from renewable resources. Prog Energy Combust Sci 2011;37(1):52–68.
[14] Eichhorn SJ, Gandini A. Materials from renewable resources. MRS Bull 2010;35(3):187–93.
[15] Nakai Y, Yoshikawa M. Cellulose as a membrane material for optical resolution. Polym J 2015;47(4):334–9.
[16] Sunilkumar M, Gafoor AA, Anas A, Haseena AP, Sujith A. Dielectric properties: a gateway to antibacterial assay—a case study of low-density polyethylene/chitosan composite films. Polym J 2014;46(7):422–9.
[17] Huang X, Zhang S, Zhang Y, Zhang H, Yang X. Sulfonated polyimide/chitosan composite membranes for a vanadium redox flow battery: influence of the sulfonation degree of the sulfonated polyimide. Polym J 2016;48(8):905–18.
[18] Rinaudo M. Chitin and chitosan: properties and applications. Prog Polym Sci 2006;31(7):603–32.
[19] Xu C, Arancon RAD, Labidi J, Luque R. Lignin depolymerisation strategies: towards valuable chemicals and fuels. Chem Soc Rev 2014;43(22):7485–500.
[20] Besson M, Gallezot P, Pinel C. Conversion of biomass into chemicals over metal catalysts. Chem Rev 2014;114(3):1827–70.
[21] Pérez S, Bertoft E. The molecular structures of starch components and their contribution to the architecture of starch granules: a comprehensive review. Starke 2010;62(8):389–420.
[22] Damager I, Engelsen SB, Blennow A, Møller BL, Motawia MS. First principles insight into the α-glucan structures of starch: their synthesis, conformation, and hydration. Chem Rev 2010;110(4):2049–80.
[23] Lligadas G, Ronda JC, Galià M, Cádiz V. Renewable polymeric materials from vegetable oils: a perspective. Mater Today 2013;16(9):337–43.
[24] Chen GQ. A microbial polyhydroxyalkanoates (PHA) based bio- and materials industry. Chem Soc Rev 2009;38(8):2434–46.
[25] Irimia-Vladu M. "Green" electronics: biodegradable and biocompatible materials and devices for sustainable future. Chem Soc Rev 2014;43(2):588–610.
[26] Tobjörk D, Österbacka R. Paper electronics. Adv Mater 2011;23(17):1935–61.
[27] Eder F, Klauk H, Halik M, Zschieschang U, Schmid G, Dehm C. Organic electronics on paper. Appl Phys Lett 2004;84(14):2673–5.
[28] Bollström R, Määttänen A, Tobjörk D, Ihalainen P, Kaihovirta N, Österbacka R, et al. A multilayer coated fiber-based substrate suitable for printed functionality. Org Electron 2009;10(5):1020–3.
[29] Zschieschang U, Yamamoto T, Takimiya K, Kuwabara H, Ikeda M, Sekitani T, et al. Organic electronics on banknotes. Adv Mater 2011;23(5):654–8.
[30] Yun TY, Eom S, Lim S. Based capacitive touchpad using home inkjet printer. J Disp Technol 2016;12(11):1411–6.
[31] Shao F, Feng P, Wan C, Wan X, Yang Y, Shi Y, et al. Multifunctional logic demonstrated in a flexible multigate oxide-based electric-double-layer transistor on paper substrate. Adv Electron Mater 2017;3(3):1600509.
[32] Ha D, Zhitenev NB, Fang Z. Paper in electronic and optoelectronic devices. Adv Electron Mater 2018;4(5):1700593.
[33] Casula G, Lai S, Matino L, Santoro F, Bonfiglio A, Cosseddu P. Printed, low-voltage, all-organic transistors and complementary circuits on paper substrate. Adv Electron Mater 2020;6(5):1901027.
[34] Martins R, Nathan A, Barros R, Pereira L, Barquinha P, Correia N, et al. Complementary metal oxide semiconductor technology with and on paper. Adv Mater 2011;23(39):4491–6.
[35] Kim DY, Steckl AJ. Electrowetting on paper for electronic paper display. ACS Appl Mater Interfaces 2010;2(11):3318–23.
[36] Siegel AC, Phillips ST, Wiley BJ, Whitesides GM. Thin, lightweight, foldable thermochromic displays on paper. Lab Chip 2009;9(19):2775–81.
[37] Hübler A, Trnovec B, Zillger T, Ali M, Wetzold N, Mingebach M, et al. Printed paper photovoltaic cells. Adv Energy Mater 2011;1(6):1018–22.
[38] Barr MC, Rowehl JA, Lunt RR, Xu J, Wang A, Boyce CM, et al. Direct monolithic integration of organic photovoltaic circuits on unmodified paper. Adv Mater 2011;23(31):3499–505.
[39] Marsh RE, Corey RB, Pauling L. An investigation of the structure of silk fibroin. Biochim Biophys Acta 1955;16(1):1–34.
[40] Hota MK, Bera MK, Kundu B, Kundu SC, Maiti CK. A natural silk fibroin protein-based transparent bio-memristor. Adv Funct Mater 2012;22(21):4493–9.
[41] Wang CH, Hsieh CY, Hwang JC. Flexible organic thin-film transistors with silk fibroin as the gate dielectric. Adv Mater 2011;23(14):1630–4.
[42] Capelli R, Amsden JJ, Generali G, Toffanin S, Benfenati V, Muccini M, et al. Integration of silk protein in organic and light-emitting transistors. Org Electron 2011;12(7):1146–51.
[43] Chang TH, Liao CP, Tsai JC, Lee CY, Hwang JC, Tso IM, et al. Natural polyelectrolyte: major ampullate spider silk for electrolyte organic field-effect transistors. Org Electron 2014;15(4):954–60.
[44] Kim DH, Viventi J, Amsden JJ, Xiao J, Vigeland L, Kim YS, et al. Dissolvable films of silk fibroin for ultrathin conformal bio-integrated electronics. Nat Mater 2010;9(6):511–7.
[45] Hwang SW, Tao H, Kim DH, Cheng H, Song JK, Rill E, et al. A physically transient form of silicon electronics. Science 2012;337(6102):1640–4.
[46] Diddens I, Murphy B, Krisch M, Müller M. Anisotropic elastic properties of cellulose measured using inelastic X-ray scattering. Macromolecules 2008;41(24):9755–9.
[47] Matsuo M, Sawatari C, Iwai Y, Ozaki F. Effect of orientation distribution and crystallinity on the measurement by X-ray diffraction of the crystal lattice moduli of cellulose I and II. Macromolecules 1990;23(13):3266–75.
[48] Sakurada I, Ito T, Nakamae K. Elastic moduli of polymer crystals for the chain axial direction. Makromol Chem 1964;75(1):1–10.
[49] Klemm D, Heublein B, Fink HP, Bohn A. Cellulose: fascinating biopolymer and sustainable raw material. Angew Chem Int Ed Engl 2005;44(22):3358–93.
[50] Oldenbourg R, Wen X, Meyer RB, Caspar DLD. Orientational distribution function in nematic tobacco-mosaic-virus liquid crystals measured by X-ray diffraction. Phys Rev Lett 1988;61(16):1851–4.
[51] Buining PA, Lekkerkerker HNW. Isotropic-nematic phase separation of a dispersion of organophilic boehmite rods. J Phys Chem 1993;97(44):11510–6.
[52] Risteen BE, Blake A, McBride MA, Rosu C, Park JO, Srinivasarao M, et al. Enhanced alignment of water-soluble polythiophene using cellulose nanocrystals as a liquid crystal template. Biomacromolecules 2017;18(5):1556–62.
[53] Liu Q, Campbell MG, Evans JS, Smalyukh II. Orientationally ordered colloidal co-dispersions of gold nanorods and cellulose nanocrystals. Adv Mater 2014;26(42):7178–84.
[54] Petritz A, Wolfberger A, Fian A, Griesser T, Irimia-Vladu M, Stadlober B. Cellulose-derivative-based gate dielectric for high-performance organic complementary inverters. Adv Mater 2015;27(46):7645–56.
[55] Thiemann S, Sachnov SJ, Pettersson F, Bollström R, Österbacka R, Wasserscheid P, et al. Cellulose-based ionogels for paper electronics. Adv Funct Mater 2014;24(5):625–34.
[56] Chiu YC, Sun HS, Lee WY, Halila S, Borsali R, Chen WC. Oligosaccharide carbohydrate dielectrics toward high-performance non-volatile transistor memory devices. Adv Mater 2015;27(40):6257–64.
[57] Chiu YC, Otsuka I, Halila S, Borsali R, Chen WC. High-performance nonvolatile transistor memories of pentacence using the green electrets of sugar-based block copolymers and their supramolecules. Adv Funct Mater 2014;24(27):4240–9.
[58] Hagenmaier RD, Shaw PE. Permeability of shellac coatings to gases and water vapor. J Agric Food Chem 1991;39(5):825–9.
[59] Goswami DN. Dielectric behavior of the constituents of the natural resin shellac. J Appl Polym Sci 1979;24(9):1977–84.

[60] Irimia-Vladu M, Głowacki ED, Schwabegger G, Leonat L, Akpinar HZ, Sitter H, et al. Natural resin shellac as a substrate and a dielectric layer for organic field-effect transistors. Green Chem 2013;15(6):1473–6.
[61] Mao LK, Hwang JC, Tsai JC. Operation voltage reduction and gain enhancement in organic CMOS inverters with the TTC/gelatin bilayer dielectric. Org Electron 2015;16:221–6.
[62] Acar H, Çınar S, Thunga M, Kessler MR, Hashemi N, Montazami R. Study of physically transient insulating materials as a potential platform for transient electronics and bioelectronics. Adv Funct Mater 2014;24(26):4135–43.
[63] Paradossi G, Cavalieri F, Chiessi E, Spagnoli C, Cowman MK. Poly(vinyl alcohol) as versatile biomaterial for potential biomedical applications. J Mater Sci Mater Med 2003;14:687–91.
[64] Chang JW, Wang CG, Huang CY, Tsai TD, Guo TF, Wen TC. Chicken albumen dielectrics in organic field-effect transistors. Adv Mater 2011;23(35):4077–81.
[65] Lu Y, Fujii M. Dielectric analysis of hen egg white with denaturation and in cool storage. Int J Food Sci Technol 1998;33(4):393–9.
[66] Surjushe A, Vasani R, Saple DG. Aloe vera: a short review. Indian J Dermatol 2008;53(4):163–6.
[67] Khor LQ, Cheong KY. Aloe vera gel as natural organic dielectric in electronic application. J Mater Sci Mater Electron 2013;24(7):2646–52.
[68] Lim ZX, Sreenivasan S, Wong YH, Zhao F, Cheong KY. Filamentary conduction in Aloe vera film for memory application. Procedia Eng 2017;184:655–62.
[69] Khor LQ, Cheong KY. N-type organic field-effect transistor based on fullerene with natural Aloe vera/SiO_2 nanoparticles as gate dielectric. ECS J Solid State Sci Technol 2013;2(11):440–4.
[70] Alberts B. Molecular biology of the cell. 5th ed. New York: Garland Science; 2008.
[71] Hinze D, Hatnik U, Sturm M. An object oriented simulation of real occurring biological processes for DNA computing and its experimental verification. In: Jonoska N, Seeman NC, editors. DNA computing. New York: Springer; 2002. p. 1–13.
[72] Church GM, Gao Y, Kosuri S. Next-generation digital information storage in DNA. Science 2012;337(6102):1628.
[73] Braich RS, Chelyapov N, Johnson C, Rothemund PWK, Adleman L. Solution of a 20-variable 3-SAT problem on a DNA computer. Science 2002;296 (5567):499–502.
[74] Reif JH. Successes and challenges. Science 2002;296(5567):478–9.
[75] Jones MR, Seeman NC, Mirkin CA. Programmable materials and the nature of the DNA bond. Science 2015;347(6224):1260901.
[76] Park SM, Park G, Cha YJ, Yoon DK. Generation of 2D DNA microstructures via topographic control and shearing. Small 2020;16(34):e2002449.
[77] Cha YJ, Park SM, You R, Kim H, Yoon DK. Microstructure arrays of DNA using topographic control. Nat Commun 2019;10(1):2512.
[78] Cha YJ, Gim MJ, Oh K, Yoon DK. Twisted-nematic-mode liquid crystal display with a DNA alignment layer. J Inf Disp 2015;16(3):129–35.
[79] Gomez EF, Venkatraman V, Grote JG, Steckl AJ. Exploring the potential of nucleic acid bases in organic light emitting diodes. Adv Mater 2015;27 (46):7552–62.
[80] Steckl AJ. DNA—a new material for photonics? Nat Photonics 2007;1(1):3–5.
[81] Hagen JA, Li W, Steckl AJ, Grote JG. Enhanced emission efficiency in organic light-emitting diodes using deoxyribonucleic acid complex as an electron blocking layer. Appl Phys Lett 2006;88(17):171109.
[82] Lee W, Chen Q, Fan X, Yoon DK. Digital DNA detection based on a compact optofluidic laser with ultra-low sample consumption. Lab Chip 2016;16 (24):4770–6.
[83] Steckl AJ, Spaeth H, You H, Gomez E, Grote J. DNA as an optical material. Opt Photonics News 2011;22(7):34–9.
[84] Gomez EF, Venkatraman V, Grote JG, Steckl AJ. DNA bases thymine and adenine in bio-organic light emitting diodes. Sci Rep 2014;4(1):7105.
[85] Malliaras G, Abidian MR. Organic bioelectronic materials and devices. Adv Mater 2015;27(46):7492.
[86] Faber C, Attaccalite C, Olevano V, Runge E, Blase X. First-principles GW calculations for DNA and RNA nucleobases. Phys Rev B Condens Matter Mater Phys 2011;83(11):115123.
[87] Lee J, Park JH, Lee YT, Jeon PJ, Lee HS, Nam SH, et al. DNA-base guanine as hydrogen getter and charge-trapping layer embedded in oxide dielectrics for inorganic and organic field-effect transistors. ACS Appl Mater Interfaces 2014;6(7):4965–73.
[88] Bravaya KB, Kostko O, Dolgikh S, Landau A, Ahmed M, Krylov AI. Electronic structure and spectroscopy of nucleic acid bases: ionization energies, ionization-induced structural changes, and photoelectron spectra. J Phys Chem A 2010;114(46):12305–17.
[89] Pong W, Inouye CS. Vacuum ultraviolet photoemission studies of nucleic acid bases. J Appl Phys 1976;47(8):3444–6.
[90] Urano S, Yang X, LeBreton PR. UV photoelectron and quantum mechanical characterization of DNA and RNA bases: valence electronic structures of adenine, 1,9-dimethyl-guanine, l-methylcytosine, thymine and uracil. J Mol Struct 1989;214:315–28.
[91] Magulick J, Beerbom MM, Schlaf R. Comparison of ribonucleic acid homopolymer ionization energies and charge injection barriers. J Phys Chem B 2006;110(32):15973–81.
[92] Bixon M, Giese B, Wessely S, Langenbacher T, Michel-Beyerle ME, Jortner J. Long-range charge hopping in DNA. Proc Natl Acad Sci USA 1999;96 (21):11713–6.
[93] Henderson PT, Jones D, Hampikian G, Kan Y, Schuster GB. Long-distance charge transport in duplex DNA: the phonon-assisted polaron-like hopping mechanism. Proc Natl Acad Sci USA 1999;96(15):8353–8.
[94] Kawai K, Kodera H, Osakada Y, Majima T. Sequence-independent and rapid long-range charge transfer through DNA. Nat Chem 2009;1(2):156–9.
[95] Meggers E, Michel-Beyerle ME, Giese B. Sequence dependent long range hole transport in DNA. J Am Chem Soc 1998;120(49):12950–5.
[96] Xiang L, Palma JL, Bruot C, Mujica V, Ratner MA, Tao N. Intermediate tunnelling-hopping regime in DNA charge transport. Nat Chem 2015;7 (3):221–6.
[97] Porath D, Bezryadin A, de Vries S, Dekker C. Direct measurement of electrical transport through DNA molecules. Nature 2000;403(6770):635–8.
[98] Lee HY, Tanaka H, Otsuka Y, Yoo KH, Lee JO, Kawai T. Control of electrical conduction in DNA using oxygen hole doping. Appl Phys Lett 2002;80 (9):1670–2.
[99] Saito I, Nakamura T, Nakatani K, Yoshioka Y, Yamaguchi K, Sugiyama H. Mapping of the hot spots for DNA damage by one-electron oxidation: efficacy of GG doublets and GGG triplets as a trap in long-range hole migration. J Am Chem Soc 1998;120(48):12686–7.
[100] Ben-Jacob E, Hermon Z, Caspi S. DNA transistor and quantum bit element: realization of nano-biomolecular logical devices. Phys Lett A 1999;263 (3):199–202.
[101] Zhang Y, Zalar P, Kim C, Collins S, Bazan GC, Nguyen TQ. DNA interlayers enhance charge injection in organic field-effect transistors. Adv Mater 2012;24(31):4255–60.
[102] Shi W, Yu J, Huang W, Zheng Y. Performance improvement of a pentacene organic field-effect transistor through a DNA interlayer. J Phys D Appl Phys 2014;47(20):205402.
[103] Watson JD, Crick FHC. Molecular structure of nucleic acids; a structure for deoxyribose nucleic acid. Nature 1953;171(4356):737–8.
[104] Lydon JE. The DNA double helix—the untold story. Liq Cryst Today 2003;12 (2):1–9.
[105] Robinson C. Liquid-crystalline structures in polypeptide solutions. Tetrahedron 1961;13(1–3):219–34.
[106] Livolant F, Levelut AM, Doucet J, Benoit JP. The highly concentrated liquid-crystalline phase of DNA is columnar hexagonal. Nature 1989;339 (6227):724–6.
[107] Rill RL, Strzelecka TE, Davidson MW, van Winkle DH. Ordered phases in concentrated DNA solutions. Phys A 1991;176(1):87–116.
[108] Merchant K, Rill RL. DNA length and concentration dependencies of anisotropic phase transitions of DNA solutions. Biophys J 1997;73 (6):3154–63.
[109] Allmann BP, Shearer PM. A high-frequency secondary event during the 2004 Parkfield earthquake. Science 2007;318(5854):1279–83.
[110] Brandes R, Kearns DR. Magnetic ordering of DNA liquid crystals. Biochemistry 1986;25(20):5890–5.
[111] Alam TM, Drobny G. Magnetic ordering in synthetic oligonucleotides. A deuterium nuclear magnetic resonance investigation. J Chem Phys 1990;92 (11):6840–6.
[112] Hagerman PJ. Flexibility of DNA. Ann Rev Biophys Biophys Chem 1988;17:265–86.
[113] Cha YJ, Yoon DK. Control of periodic zigzag structures of DNA by a simple shearing method. Adv Mater 2017;29(3):1604247.
[114] Cha YJ, Kim DS, Yoon DK. Highly aligned plasmonic gold nanorods in a DNA matrix. Adv Funct Mater 2017;27(45):1703790.
[115] Kesama MR, Dugasani SR, Cha YJ, Son J, Gnapareddy B, Yoo S, et al. Optoelectrical and mechanical properties of multiwall carbon nanotube-integrated DNA thin films. Nanotechnology 2019;30(24):245704.
[116] Han MJ, McBride M, Risteen B, Zhang G, Khau BV, Reichmanis E, et al. Highly oriented and ordered water-soluble semiconducting polymers in a DNA matrix. Chem Mater 2020;32(2):688–96.
[117] Murphy CJ, Arkin MR, Jenkins Y, Ghatlia ND, Bossmann SH, Turro NJ, et al. Long-range photoinduced electron transfer through a DNA helix. Science 1993;262(5136):1025–9.
[118] Wang L, Yoshida J, Ogata N, Sasaki S, Kajiyama T. Self-assembled supramolecular films derived from marine deoxyribonucleic acid (DNA)–cationic surfactant complexes: large-scale preparation and optical and thermal properties. Chem Mater 2001;13(4):1273–81.
[119] Catherall T, Huskisson D, McAdams S, Vijayaraghavan A. Self-assembly of one dimensional DNA-templated structure. J Mater Chem C Mater Opt Electron Devices 2014;2(34):6895–920.
[120] Heckman EM, Hagen JA, Yaney PP, Grote JG, Hopkins FK. Processing techniques for deoxyribonucleic acid: biopolymer for photonics applications. Appl Phys Lett 2005;87(21):211115.
[121] Hirata K, Oyamada T, Imai T, Sasabe H, Adachi C, Koyama T. Electroluminescence as a probe for elucidating electrical conductivity in a deoxyribonucleic acid-cetyltrimethylammonium lipid complex layer. Appl Phys Lett 2004;85(9):1627–9.
[122] Stadler P, Oppelt K, Singh TB, Grote JG, Schwödiauer R, Bauer S, et al. Organic field-effect transistors and memory elements using deoxyribonucleic acid (DNA) gate dielectric. Org Electron 2007;8(6):648–54.
[123] Kwon YW, Lee CH, Choi DH, Jin JI. Materials science of DNA. J Mater Chem 2009;19(10):1353–80.
[124] Ouchen F, Venkat N, Joyce DM, Singh KM, Smith SR, Yaney PP, et al. Deoxyribonucleic acid-ceramic hybrid dielectrics for potential application as

gate insulators in organic field effect transistors. Appl Phys Lett 2013;103(11):113701.
[125] Kim YS, Jung KH, Lee UR, Kim KH, Hoang MH, Jin JI, et al. High-mobility bio-organic field effect transistors with photoreactive DNAs as gate insulators. Appl Phys Lett 2010;96(10):103307.
[126] Yumusak C, Singh TB, Sariciftci NS, Grote JG. Bio-organic field effect transistors based on crosslinked deoxyribonucleic acid (DNA) gate dielectric. Appl Phys Lett 2009;95(26):263304.
[127] Tang CW, Albrecht AC. Photovoltaic effects of metal–chlorophyll-a–metal sandwich cells. J Chem Phys 1975;62(6):2139–49.
[128] Wang XF, Wang L, Wang Z, Wang Y, Tamai N, Hong Z, et al. Natural photosynthetic carotenoids for solution-processed organic bulk-heterojunction solar cells. J Phys Chem C 2013;117(2):804–11.
[129] Ferreira ESB, Hulme AN, McNab H, Quye A. The natural constituents of historical textile dyes. Chem Soc Rev 2004;33(6):329–36.
[130] Głowacki ED, Irimia-Vladu M, Bauer S, Sariciftci NS. Hydrogen-bonds in molecular solids—from biological systems to organic electronics. J Mater Chem B Mater Biol Med 2013;1(31):3742–53.
[131] Aakeroy CB, Seddon KR. The hydrogen bond and crystal engineering. Chem Soc Rev 1993;22(6):397–407.
[132] Desiraju GR. Reflections on the hydrogen bond in crystal engineering. Cryst Growth Des 2011;11(4):896–8.
[133] Głowacki ED, Voss G, Sariciftci NS. 25th anniversary article: progress in chemistry and applications of functional indigos for organic electronics. Adv Mater 2013;25(47):6783–800.
[134] Irimia-Vladu M, Głowacki ED, Troshin PA, Schwabegger G, Leonat L, Susarova DK, et al. Indigo—a natural pigment for high performance ambipolar organic field effect transistors and circuits. Adv Mater 2012;24(3):375–80.
[135] Głowacki ED, Leonat L, Voss G, Bodea MA, Bozkurt Z, Ramil AM, et al. Ambipolar organic field effect transistors and inverters with the natural material Tyrian Purple. AIP Adv 2011;1(4):042132.
[136] Đerek V, Głowacki ED, Sytnyk M, Heiss W, Marciuš M, Ristić M, et al. Enhanced near-infrared response of nano- and microstructured silicon/organic hybrid photodetectors. Appl Phys Lett 2015;107(8):083302.
[137] Kanbur Y, Irimia-Vladu M, Głowacki ED, Voss G, Baumgartner M, Schwabegger G, et al. Vacuum-processed polyethylene as a dielectric for low operating voltage organic field effect transistors. Org Electron 2012;13(5):919–24.
[138] Scherwitzl B, Resel R, Winkler A. Film growth, adsorption and desorption kinetics of indigo on SiO_2. J Chem Phys 2014;140(18):184705.
[139] Truger M, Roscioni OM, Röthel C, Kriegner D, Simbrunner C, Ahmed R, et al. Surface-induced phase of Tyrian Purple (6,6′-dibromoindigo): thin film formation and stability. Cryst Growth Des 2016;16(7):3647–55.
[140] Klimovich IV, Leshanskaya LI, Troyanov SI, Anokhin DV, Novikov DV, Piryazev AA, et al. Design of indigo derivatives as environment-friendly organic semiconductors for sustainable organic electronics. J Mater Chem C Mater Opt Electron Devices 2014;2(36):7621–31.
[141] Pitayatanakul O, Higashino T, Kadoya T, Tanaka M, Kojima H, Ashizawa M, et al. High performance ambipolar organic field-effect transistors based on indigo derivatives. J Mater Chem C Mater Opt Electron Devices 2014;2(43):9311–7.
[142] Klebe G, Graser E, Hädicke E, Berndt J. Crystallochromy as a solid-state effect: correlation of molecular conformation, crystal packing and colour in perylene-3,4:9,10-bis(dicarboximide) pigments. Acta Crystallogr Sect B 1989;B45(1):69–77.
[143] Hunger K. Toxicology and toxicological testing of colorants. Rev Prog Color Relat Top 2005;35(1):76–89.
[144] Głowacki ED, Irimia-Vladu M, Kaltenbrunner M, Gsiorowski J, White MS, Monkowius U, et al. Hydrogen-bonded semiconducting pigments for air-stable field-effect transistors. Adv Mater 2013;25(11):1563–9.
[145] Haucke G, Graness G. Thermal isomerization of indigo. Angew Chem Int Ed Engl 1995;34(1):67–8.
[146] Głowacki ED, Romanazzi G, Yumusak C, Coskun H, Monkowius U, Voss G, et al. Epindolidiones-versatile and stable hydrogen-bonded pigments for organic field-effect transistors and light-emitting diodes. Adv Funct Mater 2015;25(5):776–87.
[147] Rossi L, Bongiovanni G, Kalinowski J, Lanzani G, Mura A, Nisoli M, et al. Ultrafast optical probes of electronic excited states in linear trans-quinacridone. Chem Phys Lett 1996;257(5–6):545–51.
[148] Labana SS, Labana LL. Quinacridones. Chem Rev 1967;67(1):1–18.
[149] McGinness J, Corry P, Proctor P. Amorphous semiconductor switching in melanins. Science 1974;183(4127):853–5.
[150] Bothma JP, de Boor J, Divakar U, Schwenn PE, Meredith P. Device-quality electrically conducting melanin thin films. Adv Mater 2008;20(18):3539–42.
[151] Ambrico M, Ambrico PF, Cardone A, Ligonzo T, Cicco SR, Di Mundo R, et al. Melanin layer on silicon: an attractive structure for a possible exploitation in bio-polymer based metal-insulator-silicon devices. Adv Mater 2011;23(29):3332–6.
[152] Bettinger CJ, Bruggeman JP, Misra A, Borenstein JT, Langer R. Biocompatibility of biodegradable semiconducting melanin films for nerve tissue engineering. Biomaterials 2009;30(17):3050–7.
[153] Ambrico M, Cardone A, Ligonzo T, Augelli V, Ambrico PF, Cicco S, et al. Hysteresis-type current-voltage characteristics in Au/eumelanin/ITO/glass structure: towards melanin based memory devices. Org Electron 2010;11(11):1809–14.
[154] Lin YJ. Hysteresis-type current-voltage characteristics of indium tin oxide/poly(3,4-ethylenedioxythiophene) doped with poly(4-styrenesulfonate)/indium tin oxide devices. J Appl Phys 2008;103(6):063702.
[155] Zhong C, Deng Y, Roudsari AF, Kapetanovic A, Anantram MP, Rolandi M. A polysaccharide bioprotonic field-effect transistor. Nat Commun 2011;2(1):476.
[156] Angione MD, Pilolli R, Cotrone S, Magliulo M, Mallardi A, Palazzo G, et al. Carbon based materials for electronic bio-sensing. Mater Today 2011;14(9):424–33.
[157] Muskovich M, Bettinger CJ. Biomaterials-based electronics: polymers and interfaces for biology and medicine. Adv Healthc Mater 2012;1(3):248–66.
[158] Serrano MC, Chung EJ, Ameer GA. Advances and applications of biodegradable elastomers in regenerative medicine. Adv Funct Mater 2010;20(2):192–208.
[159] Sekitani T, Someya T. Human-friendly organic integrated circuits. Mater Today 2011;14(9):398–407.
[160] Irimia-Vladu M, Sariciftci NS, Bauer S. Exotic materials for bio-organic electronics. J Mater Chem 2011;21(5):1350–61.
[161] Khodagholy D, Doublet T, Gurfinkel M, Quilichini P, Ismailova E, Leleux P, et al. Highly conformable conducting polymer electrodes for *in vivo* recordings. Adv Mater 2011;23(36):H268–72.
[162] Abidian MR, Ludwig KA, Marzullo TC, Martin DC, Kipke DR. Interfacing conducting polymer nanotubes with the central nervous system: chronic neural recording using poly(3,4-ethylenedioxythiophene) nanotubes. Adv Mater 2009;21(37):3764–70.
[163] Richardson-Burns SM, Hendricks JL, Martin DC. Electrochemical polymerization of conducting polymers in living neural tissue. J Neural Eng 2007;4(2):L6–13.
[164] Luo SC, Mohamed Ali E, Tansil NC, Yu HH, Gao S, Kantchev EAB, et al. Poly(3,4-ethylenedioxythiophene) (PEDOT) nanobiointerfaces: thin, ultrasmooth, and functionalized PEDOT films with *in vitro* and *in vivo* biocompatibility. Langmuir 2008;24(15):8071–7.
[165] Isaksson J, Kjäll P, Nilsson D, Robinson ND, Berggren M, Richter-Dahlfors A. Electronic control of Ca^{2+} signalling in neuronal cells using an organic electronic ion pump. Nat Mater 2007;6(9):673–9.
[166] Bolin MH, Svennersten K, Wang X, Chronakis IS, Richter-Dahlfors A, Jager EWH, et al. Nano-fiber scaffold electrodes based on PEDOT for cell stimulation. Sens Actuators B Chem 2009;142(2):451–6.
[167] Tybrandt K, Larsson KC, Kurup S, Simon DT, Kjäll P, Isaksson J, et al. Translating electronic currents to precise acetylcholine-induced neuronal signaling using an organic electrophoretic delivery device. Adv Mater 2009;21(44):4442–6.
[168] Tybrandt K, Larsson KC, Richter-Dahlfors A, Berggren M. Ion bipolar junction transistors. Proc Natl Acad Sci USA 2010;107(22):9929–32.
[169] Torsi L, Farinola GM, Marinelli F, Tanese MC, Omar OH, Valli L, et al. A sensitivity-enhanced field-effect chiral sensor. Nat Mater 2008;7(5):412–7.
[170] George PM, Lyckman AW, LaVan DA, Hegde A, Leung Y, Avasare R, et al. Fabrication and biocompatibility of polypyrrole implants suitable for neural prosthetics. Biomaterials 2005;26(17):3511–9.